

# Impact of climate change on precipitation in Suriname

## Master Thesis

**Jacob Smit**

Student number: 4585860

Date: July 2023

Supervisors: Dr. M.M. Rutten, TU Delft, chair  
Dr. R.J. van der Ent, TU Delft  
Dr. R. Haarsma, KNMI

## Abstract

Suriname is highly vulnerable to hazards that are climate change related, such as droughts and floods. Knowledge about future precipitation in Suriname is needed for the population of Suriname in order to adapt to climate change effects. By analysing 32 CMIP6 models, this study investigates the impact of climate change on precipitation in Suriname. The intermodel spread of the projected change in precipitation in 2100 compared to the reference period (1991-2020) is large, ranging from -45% (-2.0 mm/day) to +10% (+0.5 mm/day). Drivers of climate change in Suriname are the Intertropical Convergence Zone (ITCZ), Atlantic Meridional Overturning Circulation (AMOC) and El Niño Southern Oscillation (ENSO). A weaker AMOC strength leads to warming of the south Atlantic Ocean and cooling of the north Atlantic Ocean, indicating a southward shift of the ITCZ. More El Niño like conditions lead to weakening of the mean zonal circulation along the equator and an eastward migration of the Walker Circulation in the Pacific. The occurrence of an increase in upward motion over the Pacific ITCZ and an increase in downward motion over Suriname also indicate an eastward migration of the Walker Circulation. With an eastward migrated Walker circulation an upward motion of moisture is strengthened and deep convection is increased over the Pacific. At the same time the opposite happens in Suriname where deep convection is decreased due to downward motion of air.

Models with relatively high future drying project the ITCZ at a more southward position, leading to low precipitation amounts in Suriname. Next to that, these models project a relatively stronger southward shift of the ITCZ compared to wet models, leading to an even stronger drying effect in Suriname. The climate models show a mean weakening of the AMOC strength, especially the dry models. More El Niño like conditions, with a decrease in deep convection in projections from dry models, are another reason for lower precipitation projections for dry models than for wet models.

After a bias-correction with Quantile Delta Mapping (QDM) the intermodel spread decreases significantly from 1-8 mm/day to 4-7.5 mm/day. Next to that, QDM correction has shifted the historical multimodel mean precipitation upwards by approximately 3 mm/day, almost doubling it. The doubling of the average precipitation indicates that climate models fail to accurately simulate the climate in Suriname. The 10% most extreme 1-day and 5-day cumulative precipitation values decrease according to climate projections. This is probably due to a decrease in the average projected precipitation in Suriname throughout the year. Extreme precipitation increases for the 0.1% most extreme 1-day and 5-day cumulative precipitation values. Despite the projected decrease in average precipitation, the models project more intense extreme precipitation events. The higher values for 0.1% extreme events can be explained by future warming, giving rise to a higher air capacity for water vapor.

## Table of Contents

1. Introduction.....	1
1.1. Motivation.....	1
1.2. Research purpose & questions.....	3
2. Suriname description .....	4
2.1. Climate and characteristics .....	4
2.2. Climate drivers.....	5
3. Materials and methods .....	9
3.1. Materials.....	9
3.2. Methods .....	10
4. Results .....	14
4.1. Climatology.....	14
4.2. Precipitation bias.....	14
4.3. Climate drivers of Suriname .....	17
4.4. Dry and wet models .....	18
4.5. April & May.....	22
4.6. Atlantic Meridional Overturning Circulation (AMOC) .....	23
4.7. Coast and inland .....	23
4.8. Quantile Delta Mapping .....	24
4.9. Extreme precipitation.....	26
5. Discussion.....	27
6. Conclusion .....	32
References.....	35
A Supplementary Figures.....	39
B Supplementary Tables.....	47

# 1. Introduction

## 1.1. Motivation

Suriname is one of the Small Island Developing States (SIDS) (Solaun et al., 2021). These states are highly vulnerable to hazards that are climate change related. The inhabitants are at risk due to droughts, flooding and erosion at the coast. The population relies financially on fragile infrastructure and local markets of agriculture and fishing. Climate change is expected to increase the frequency of natural hazards in these territories the inhabitants rely on, while simultaneously causing damage to the ecosystem. This could have a huge impact on agriculture, water availability, water drainage, forestry and infrastructure, resulting in a reduction of traditional employment. (Antich-Homar et al., 2022).

Climate change in Suriname is influenced by multiple mechanisms (Figure 1) that might not be adequately represented in the climate models, resulting in inaccurate and/or highly variable projections. These are mechanisms such as El Niño Southern Oscillation (ENSO) (Köhl et al., 2022), the Inter Tropical Convergence Zone (ITCZ) (Nurmohamed et al., 2007), the Atlantic Meridional Overturning Circulation (AMOC) (Nurmohamed et al., 2008), Pacific Walker circulation (Andreoli et al., 2017) and changes in convergence of moisture over Suriname (Vasconcellos et al., 2020). Previous studies like Da Rocha et al. (2009), Karmalkar et al. (2011), Llopart et al. (2017) and Vasconcellos et al. (2020) have already shown that climate models simulations for the current climate compared to observations have negative precipitation biases for the north of South-America and Central America.

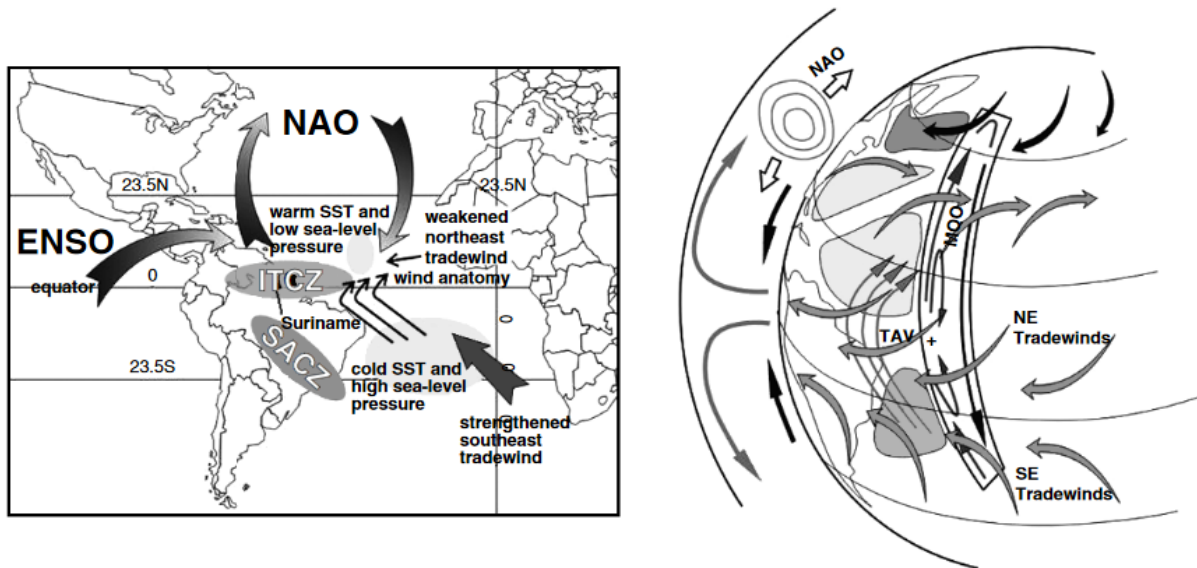


**Figure 1:** Atmospheric and oceanic mechanisms influencing the climate in Suriname (Nurmohamed et al., 2007).

Earlier studies suggest that due to a shorter projected ITCZ seasonal cycle over Suriname, the rainfall distribution in the rainy season is expected to become concentrated in fewer months (Antich-Homar et al., 2022). The rainy season will become concentrated in fewer months leading to a decrease in the amount of rainfall days. At the same time the number of extreme precipitation events increases. As a result the amount of rainfall in one day and in five consecutive days is expected to increase. Suriname is vulnerable to extreme rainfall events because the infrastructure is not resistant to extreme rainfall events. River floods are already a big problem for Suriname and this will become an even greater risk in the future (Weekes and Bello, 2019). Extreme precipitation needs to be researched more accurately with statistically downscaled models. Analysis can be done on the

extreme precipitation and afterwards this could potentially be used for taking action in preventing disasters like river floods.

To investigate the impact of climate change for Suriname the output of the Coupled Modelling Intercomparison Project Phase 6 (CMIP6) is used. CMIP6 consists of Global Climate Models (GCMs) that use historical data to simulate future climate projections (CMIP Phase 6, 2020). Thirty-two of those GCMs will be used in this study. The simulations are used to show how climate systems responds to different scenarios of radiative forcing. An increase in carbon dioxide emissions causes a higher radiative forcing. The different scenarios are called Shared Socio-economic Pathways (SSP). In this study the “middle of the road” emission scenario SSP2-4.5 and high emission scenario SSP5-8.5 are taken as CMIP6 forcing scenarios. Currently, the CMIP6 models show a large spread in the projected change (-45% to +10% in 2100) in rainfall over Suriname ranging from a small to a large decrease (Figure 2). This means that there is a large uncertainty between the different models.

State of the Climate Report: Suriname from Solaun et al. (2021) is a study that has already looked at future climate change and future change in extreme rainfall in Suriname by using climate models from CMIP6. However, only three climate models were used here, while 32 models will be used in this study. The higher amount of models will give a better insight in the spread and reliability of the climate projections.

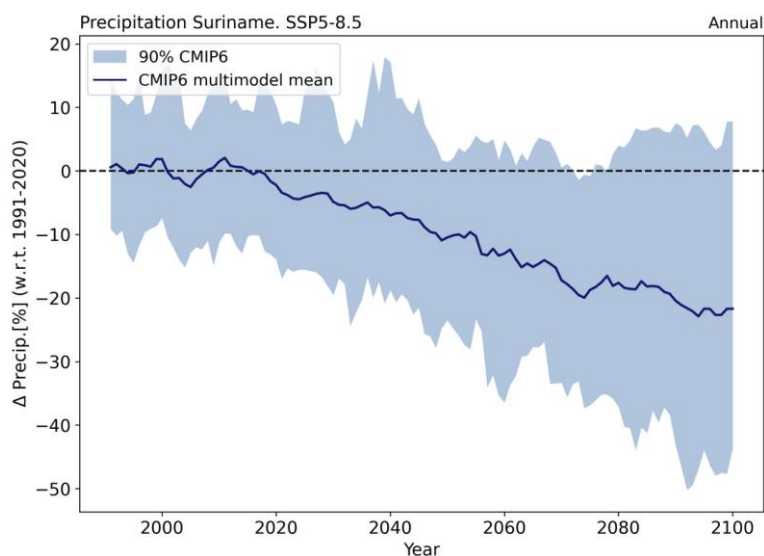


**Figure 2:** Change in annual precipitation for Suriname relative to 1991-2020 average, for the SSP5-8.5 scenario. The shaded area is the 90% intermodel spread.

The reasons for the differences in historical climate projections between climate models and observed data need to be analysed. The current climate models could be improved if the causes for its biases can be determined. Biases have already been reduced in the CMIP6 models with respect to CMIP5 (Ortega et al., 2021). However, there are still model biases present in CMIP6 models. One way of adjusting models to their biases is using statistical downscaling with observations. There are many statistical downscaling methods. Some examples are: linear interpolation, spatial disaggregation, bias-correction and spatial disaggregation, quantile mapping, detrended quantile mapping and quantile delta mapping (Wood et al., 2004). With statistical downscaling local weather data is used to downscale a climate model to a higher resolution (Wilby and Dawson, 2013). A statistical relationship is made between historic climate observations and data of a climate model in that same period. The statistical downscaling happens in combination with a bias removal. Another kind of downscaling is dynamical downscaling. With dynamical downscaling a higher resolution climate model is used.

These models use global climate models as boundary conditions and physical principles to reproduce local climate. Dynamical downscaling is computationally expensive, but very accurate in representing physical principals. Statistical downscaling is cheap, however it can lead to physically unrealistic results (*Climate Model Downscaling – Geophysical Fluid Dynamics Laboratory, n.d.*).

## 1.2. Research purpose & questions

Climate change will affect Suriname in multiple ways. Accurate predictions and simulations of the future are needed to make it possible for the population of Suriname to adapt to effects of climate change. This way the country can be prepared to find solutions for potential climate change related problems.

The following research questions will be answered:

1. How well do climate models simulate the climate and observed trends of Suriname?
2. Which atmospheric processes influence the climate of Suriname?
3. What are the causes for the intermodel spread in projected precipitation for Suriname?
4. How reliable are the CMIP6 climate projections considering their ability to simulate the actual climate and trends of Suriname and its drivers?
5. What are the climate projections for Suriname with respect to downscaled extreme precipitation?

This thesis is structured as follows. A description of Suriname with its climate and characteristics, along with the climate drivers in Suriname, is given in Section 2. Section 3 describes the materials and methods used in this study. In Section 4 the results are given and analysed for the climatology in Suriname, the precipitation bias, climate drivers, the differences between dry and wet models, AMOC correlations, QDM corrected climate models and extreme precipitation. The results are discussed in Section 5. Finally, a conclusion is made about the impact of climate change on precipitation in Suriname, by answering the research questions.

## 2. Suriname description

### 2.1. Climate and characteristics

Suriname is a country on the north coast of South-America and borders with Brazil, Guyana and French-Guiana (Figure 3). The country was a colony of the Netherlands from 1667 to 1954 and became independent in 1975. They have a population of 613.000 people (in 2021) and the total land area is 163.820 km<sup>2</sup> (Climate Change Knowledge Database Suriname, n.d.; Wikipedia, 2023).



**Figure 3:** Geographical location Suriname. By Rei-artur - <https://commons.wikimedia.org/wiki/File:LocationSuriname.svg>, CC BY-SA 4.0, <https://commons.wikimedia.org/w/index.php?curid=123486730>

Suriname has a tropical climate with a mean temperature of 27 degrees Celsius (*Het klimaat van Suriname, n.d.*). The northern half of Suriname has a tropical rainforest climate, the southern half has a tropical monsoon climate and the mountain areas in the south of Suriname have a tropical savannah climate. Suriname does not have the seasons winter, spring, summer and autumn. Instead, there is a dry season and a wet season. Figure 8 shows the historical mean precipitation in mm per day in Suriname for the different months of the year for the period 1991-2020. Approximately, the wet season is from January until July and the dry season is from August until December. The mean total precipitation per year is 2200 mm.

High temperatures in combination with large amounts of precipitation cause a relatively high humidity, most of the times being between 80 and 95%. The dense forests in Suriname also contribute to the high relative humidity. Moisture ends up in the air through evaporation in the forests. Suriname has a high forest area with 93% of the total land area being forests.

Suriname is not in danger of hurricanes because it is located too close to the equator. However, large wind gusts occur regularly during heavy precipitation events.

## 2.2. Climate drivers

The climate of Suriname is influenced by multiple mechanisms. These mechanisms cause seasonal and interannual variability in Suriname. Changes in these mechanisms could lead to a change in the climate of Suriname. In this section the most important drivers of the climate of Suriname are introduced.

### ***Intertropical Convergence Zone (ITCZ)***

The most intense rainfall on earth, 32% of global precipitation, occurs in the Intertropical Convergence Zone (ITCZ), a narrow belt of deep convective clouds. Surface winds converge in the ITCZ, leading ascending air masses and precipitation from convective clouds (Schneider et al., 2014).

The ITCZ impacts climate and society in the tropics, moving north and south across the equator as it follows the seasonal cycle of solar insolation (Byrne et al., 2018). The Atlantic ocean transports energy northward, making the Northern Hemisphere warmer than the Southern Hemisphere. This is why the ITCZ mean position is north of the Equator in the Atlantic. On average the ITCZ is centred around six degrees north of the Equator. From July to November the ITCZ is located north of Suriname and from February to April it is located south of Suriname (Müller et al., 2012). In these months Suriname has the least precipitation.

Climate models project the highest annual precipitation in areas in the ITCZ (Llopart et al., 2017). Comparison between observations and historical simulations from climate models show that for Suriname the annual precipitation is lower in the historical simulations than the observations (Vasconcellos et al., 2020).

### ***Atlantic Meridional Overturning Circulation (AMOC)***

The Atlantic Meridional Overturning Circulation is a mechanism consisting of multiple processes: Transport of volume from the depth to near the ocean surface, light water transport toward high latitudes by surface currents, deep water formation in regions where waters become denser and sink, and deep currents closing the loop (Kuhlbrodt et al., 2007). Figure 4 shows the thermohaline circulation with warm surface flow from the south Atlantic to the north Atlantic and cool subsurface flow from the north Atlantic to the south Atlantic. The AMOC has an impact on climate through its heat and freshwater transports. Heat transport from the north Atlantic by the AMOC causes a relative warmth of the Northern Hemisphere compared to the Southern Hemisphere and is thought to have an influence on the mean position of the ITCZ being at the north of the equator (Buckley and Marshall, 2016).

In climate models simulations the AMOC strength is projected to decline. Models with a large AMOC strength decline project a southward shift of the ITCZ (Bellomo et al., 2021).



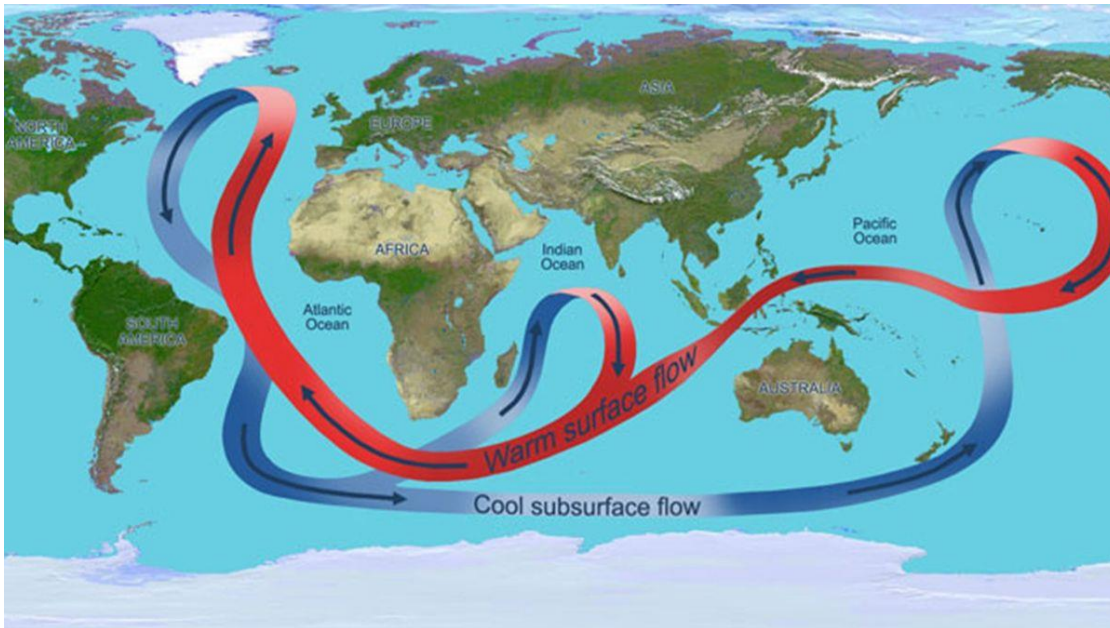


**Figure 4:** Thermohaline circulation. Warm surface flow from south Atlantic to north Atlantic and cool subsurface flow from north Atlantic to south Atlantic. (*The Collapse of a Major Atlantic Current Would Cause Worldwide Disasters, n.d.*)

AMOC strength is used to express volume transport in ocean currents (Srokosz and Bryden, 2015). The unit used for AMOC strength expression is Sverdrup. One Sverdrup is equal to one million  $\text{m}^3/\text{s}$ . Figure 5 shows AMOC strength from 1850 to 2100 with 1900-1949 as reference period. The figure shows 28 models with available information on AMOC strength. In the figure, a large intermodel spread is visible for both emission scenarios. The large differences between models in AMOC strength projection could be partly responsible for the different precipitation projections by the models, as the AMOC strength influences the mean position of the ITCZ (Zhuravleva et al., 2021).

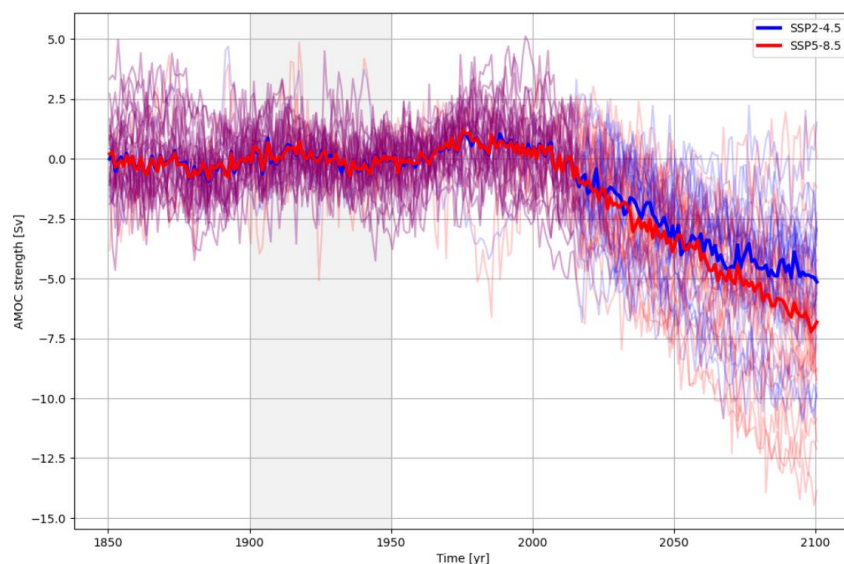


**Figure 5:** Yearly AMOC data in Sv [ $10^6 \text{ m}^3/\text{s}$ ] at  $26^\circ\text{N}$  for 28 CMIP6 models from 1850 - 2100 (historical period and scenarios SSP2-4.5 and SSP5-8.5). Reference period is 1900-1949. The solid line represents the multimodel mean.



uncertainty about the future change in ENSO. Firstly, there are large natural variations in the NAO on timescales of decades, which can mask the effect of long-term climate change on the NAO. Secondly there is a high variability between models in representing physical processes, which can lead to different projected climates (McKenna and Maycock, 2021).

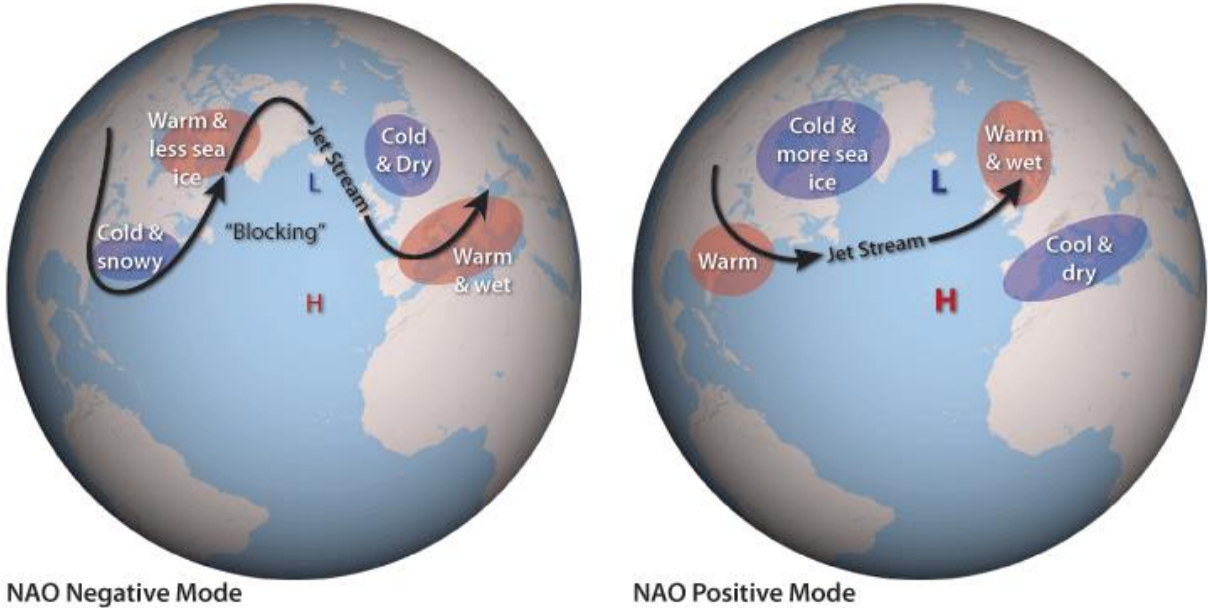


**Figure 7:** On average, the surface pressure near Iceland is relatively low (L), while the pressure near the Azores Island is relatively high (H). During a negative phase (left), this pressure difference weakens. During a positive phase (right), the difference becomes even stronger than usual. The variation in pressure patterns influences the strength and location of the jet stream and the path of storms across the North Atlantic. (Climate Variability: North Atlantic Oscillation, 2009)

## 3. Materials and methods

### 3.1. Materials

#### Observations

Historical data of the relevant variables temperature, wind and precipitation comes from Climatic Research Unit (CRU), Climate Hazards Group InfraRed Precipitation (CHIRPS), Global Precipitation Climatology Project (GPCP) and local weather stations. GPCP will be the most used observational data because this is data for the whole earth whereas the other observations only have data available for land areas.

Weather stations are reliable and therefore they are used as a reference for the real precipitation values. CRU data consists of interpolated observations, CHIRPS data consists of rain gauges and satellite observations, and GPCP has data from rain gauge stations, satellites and sounding observations merged together. Cultuurtuin is a weather station in Paramaribo with reliable precipitation observations. The Cultuurtuin dataset contains daily precipitation observations from 1852 to 2006. This data was made available by Suriname to the KNMI. There is more certainty about the reliability of observations when multiple observational sources are being used and compared. This helps to get a better understanding of differences between observations and models. The temporal resolution in the gridded datasets is a day or a month. The GPCP dataset has values from 1979 until present and a  $2.5^\circ \times 2.5^\circ$  resolution. The CRU dataset has a  $0.5^\circ \times 0.5^\circ$  resolution and CHIRPS has a  $0.05^\circ \times 0.05^\circ$  resolution.

The approximate coordinates for Suriname are: longitude:  $2-6^\circ \text{N}$  and latitude:  $54-58^\circ \text{W}$  (with 1 degree being equal to 111.1 km). This makes a total area of  $4^\circ \times 4^\circ$  for Suriname.

#### Models

Climate projections are made with the General Circulation Models used in CMIP6 (CMIP Phase 6, 2020). CMIP6 data was downloaded from the ESGF nodes (cmip6 Data Search, n.d.). This is the principal location where CMIP6 data is stored. The data is downloaded to the Surfsara Virtual Machine, a computational environment where all modelling and experiments will be performed. This data is available with different grid sizes for every climate model. A total of 32 models are used. The resolution of the CMIP6 models used in this study are listed in Figure S.2 (Supplementary Figures). Climate simulations are available from 1850 to 2100, allowing comparison between historical simulations and historical observations, and comparison between historical simulations and simulations of the future.

The analysed variables provided by climate models are: precipitation, (near surface air) temperature, wind and omega. Omega is the tendency of air pressure and plays a role in the upward component of air velocity when air pressure is being used as the vertical coordinate (*CMIP5 Atmospheric Variables — IPCC-DDC at DKRZ Documentation*, n.d.-b). A negative value indicates an upwards vertical air velocity.

Another analysed variable is the AMOC strength. There are 28 models providing AMOC strength data at  $26^\circ \text{N}$  in the North Atlantic. The reason for this specific location is because here the AMOC strength is being observed (McCarthy, 2015). As a result, model projections can be compared with these observations, such as observations from the RAPID array. RAPID is a research programme with instruments measuring AMOC strength (Hirschi et al., 2013).

## 3.2. Methods

### CMIP6 dynamics analysis

Simulations from CMIP6 models are used for dynamic analysis. Only emission scenarios SSP2-4.5 and SSP5-8.5 are analysed. However, the results are only shown for SSP5-8.5 because this scenario has more extreme changes in projections, giving the best view of differences when comparisons are made between models, groups of models and/or time. According to Tebaldi and Arblaster (2014) temperature and precipitation patterns in CMIP models only slightly change under increasing or decreasing concentrations of greenhouse gases. This is called pattern scaling, first proposed by Santer et al. (1990).

For analysing changes in time in atmospheric dynamics or variables the reference period is 1991 to 2020 and the future period is 2071 to 2100. According to the World Meteorological Organization, 30 years is the classical period for averaging variables, such as temperature, precipitation and wind (Matthews, 2018).

Atmospheric dynamics change throughout the year, giving Suriname different seasons. In this study a “wet” season (January-July) and a “dry” season (August-December) have been analysed. The dry and wet season are based on the amount of precipitation per month, described in section 4.1.

### Preprocessing models

Models are preprocessed before computations because climate models have differences in time (calendar format), latitude, longitude, units and other definitions. The grid sizes are regridded to a 1° x 1° resolution for every model in order to allow comparison between models. The regridding is done with climate data operators (cdo) tools using the bilinear interpolation method. Bilinear interpolation is a method for interpolating functions with two variables using repeated linear interpolation (Mastylo, 2013). With cdo bilinear grid interpolation the distance weighted average of the four nearest pixel values are used to estimate a new pixel value (*Regridding Overview | Climate Data Guide*, n.d.). Differences in time or display of time between models are corrected in Python by assigning the same calendar format and time period to every model. Likewise, corrections are also made to differences in units, variable names and coordinates.

### Variables

Precipitation is the main variable that will be researched in this study. However, temperature, omega and wind will also be investigated to help explain the simulated mechanisms by climate models that are driving the climate in Suriname. When climate models are being compared, precipitation change will be transformed into precipitation change scaled over mean temperature change. Variables are being scaled by the mean temperature change over the region 40°S-40°N for every model, in the same time period as the time period the variable is being calculated, to remove the effect of different climate sensitivities. The change in a scaled variable gives the change in a variable for every 1 °C temperature increase. Climate sensitivities arise because for equal increase in CO<sub>2</sub>, some models have a different warming. Different analyses on precipitation change, like absolute/relative precipitation change, precipitation differences between models or change in time, can clarify the drivers of those precipitation changes and the differences between areas, seasons and models. The mathematical variable scaling expression, for example for scaled precipitation, is shown in equation 1

$$\Delta P_{scaled} = \frac{\Delta P}{\Delta T_{40^{\circ}S-40^{\circ}N}} \quad (1)$$

Where  $\Delta P$  expresses the change in precipitation and  $\Delta T_{40^{\circ}S-40^{\circ}N}$  is the change in temperature averaged over the region 40°S-40°N.

### **Models analyses**

The model projections accuracy can be determined by comparing climate models with observations. We look at biases from the models to conclude if models are accurate in projecting intensity and position of precipitation events. The climate models precipitation bias analyses is discussed in section 4.3.

The significance of the multimodel mean difference between groups is determined by a two-tailed student t-test. A computed difference is regarded significant at the 95% confidence level. When differences between groups of models or differences between future and history are conducted, the same two-tailed student t-test will be applied.

### **Climate drivers of Suriname**

By looking at the multimodel change in time for different variables on a large spatial scale, we can find out which atmospheric and oceanic processes have an impact on the climate of Suriname. The change in time is denoted by the difference between the future and a reference period: 2085 (the average of 2071-2100) - 2005 (the average of 1991-2020). The scale of the area under study has been chosen in the way that changes in atmospheric processes that can have an influence on the climate in Suriname are within this area. The selected domain is 30°S-80°N and 160°E-360°E.

### **Dry models and wet models**

To find out what causes the intermodel spread in precipitation projection, models are categorized into different groups. This will provide insights into the different ways different models project the change in climate of Suriname and also how mechanisms that influence Suriname are simulated differently.

### **AMOC**

The AMOC analyses is done with the provided model data on AMOC strength. Figure 5 showed the projected AMOC strength from 1850 to 2100 by climate models. The AMOC strength information is used to analyse the correlation between change in AMOC strength and change in temperature, and the correlation between change in AMOC strength and change in precipitation. Pearson correlations provide p-values to quantitatively show how strong the correlations are. The results are shown in Section 4.6.

## Quantile Delta Mapping

Time series of CMIP models are transformed into bias-corrected CMIP models by using Quantile Delta Mapping (QDM) with observational datasets. A python package is used to compute the quantiles for the time series emerged from QDM. The python package is called `sdba.QuantileDeltaMapping`. QDM is a bias correction algorithm used to correct for systematic distributional biases in precipitation from climate models and is differing from other types of quantile mapping by explicitly preserving relative changes in precipitation quantiles (Cannon, 2018). First, all projected future quantiles from a model are detrended to correct systematic distributional biases relative to the observations taken as the historical baseline and then quantile mapping is applied to the detrended series. After that, the projected trends in the model quantiles are reintroduced on top of the bias-corrected outputs, to make sure the climate sensitivity of a climate models is not affected by the bias correction (Cannon et al., 2015). With QDM the cumulative distribution function (CDF) is incorporated and adjusted for the projection period on the basis of the difference between the model and observational CDFs (Li et al., 2010). The result is that all historical QDM corrected climate model CDFs are resembling the CDF from the observation time series.

QDM can be expressed in mathematical equations by following the process below from Cannon et al. (2015). QDM starts with a time-dependent CDF of the climate model projected series  $x_{m,p}$ , for example as estimated from the empirical CDF over a time window around  $t$ :

$$\tau_{m,p}(t) = F_{m,p}^{(t)}[x_{m,p}(t)], \tau_{m,p}(t) \in \{0,1\}, \quad (2)$$

where  $\tau_{m,p}(t)$  is the nonexceedance probability associated with the value at time  $t$ . The corresponding modelled  $\tau_{m,p}$  quantile in the historical period can be found by entering this value into the historical inverse CDF  $F_{m,h}^{-1}$ . The relative change in quantiles between the historical period and time  $t$  is then given by

$$\Delta_m(t) = \frac{F_{m,p}^{(t)-1}[\tau_{m,p}(t)]}{F_{m,h}^{-1}[\tau_{m,p}(t)]} = \frac{x_{m,p}(t)}{F_{m,h}^{-1}[\tau_{m,p}(t)]} \quad (3)$$

The modelled  $\tau_{m,p}$  quantile at time  $t$  can be bias corrected by applying the inverse CDF estimated from observed values  $x_{o,h}$  over the historical period

$$\hat{x}_{o:m,h:p}(t) = F_{o,h}^{-1}[\tau_{m,p}(t)] \quad (4)$$

Finally, the bias-corrected future projection at time  $t$  is given by applying the relative change  $\Delta_m(t)$  multiplicatively to this historical bias-corrected value,

$$\hat{x}_{m,p}(t) = \hat{x}_{o:m,h:p}(t)\Delta_m(t) \quad (5)$$

To preserve absolute instead of relative changes in quantiles, Equations (3) and (4) can simply be applied additively rather than multiplicatively.

In this study QDM is only done for Paramaribo. Precipitation data from the weather station in Cultuurtuin, Paramaribo is used as a reference for Quantile Delta Mapping. Precipitation data for the grid point closest to Paramaribo is chosen to be quantile delta mapped.

Analysing CMIP multimodel mean QDM corrected time series shows how the corrected models project precipitation in the future and how it differs from the original time series in terms of absolute and relative values.

Another way of analysing original and QDM corrected time series is by comparing the cumulative distribution functions. CDFs are made for the reference observations, CMIP historical, CMIP future, CMIP QDM historical and CMIP QDM future. Also, the CDFs of different observational datasets are compared to critically determine whether the choice of the reference observation being used influences the bias correction.

The QDM data is made with datasets of daily precipitation values. Then, the daily values are grouped by year to construct the time series. The CDFs are made with daily values because when the 30-year datasets are represented with monthly values, the amount of values is too small to make a clear, smooth CDF.

### **Extreme precipitation**

Extreme precipitation analyses is done with regard to dangers like floods. The 10%, 5%, 1% and 0.1 quantiles of 1-day and 5-day cumulative precipitation are computed for climate models and for the QDM corrected climate models, for scenarios SSP2-4.5 and SSP5-8.5. Then the relative and absolute changes for the future period (2071-2100) compared to the reference period (1991-2020) are calculated. This is done annually, in the dry season and the wet season, for all models, dry models and wet models. All days, including days without precipitation, are included in the calculations.

First the values for the different extremes are calculated using the code `quantile()`, a method in Pandas. For example, the 1% extreme is calculated by using `quantile(0.99)`. After all extremes have been calculated, the change in precipitation extremes is computed separately for each model. Then the average is calculated of model changes in extremes, per extreme, for every model group.



## 4. Results

### 4.1. Climatology

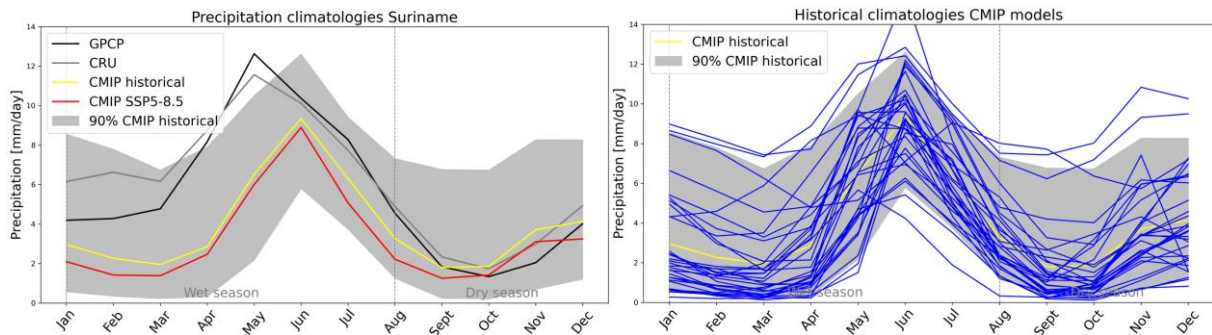


**Figure 8:** Left figure: Monthly precipitation for Suriname in mm/day for GPCP and CRU observations (1991-2020), CMIP historical multimodel mean (1991-2020), CMIP SSP5-8.5 multimodel mean (2071-2100) and the 90% CMIP model mean spread (1991-2020). Right figure: the historical mean for all CMIP models.

The GPCP and CRU observations both show high precipitation in the months March to July and low precipitation from August to November (Figure 8, left). Both observational datasets have a similar progression throughout the year apart from the higher values for CRU in the first 3 months of the year. The CMIP historical model mean has a strong negative bias in the first half of the year, with p-values ranging from  $1.5e-13$  to 0.02, and a positive bias in November with p-value = 0.004. The model projections only match the observations in September, October, and December. The multimodel mean SSP5-8.5 (Figure 8, left) is lower than the historical CMIP multimodel mean for every month but the difference between the two multimodel means is only significant (p-value smaller than 0.05) in four months. All p-values for the models historical vs models future and models historical and GPCP, are listed in Table B.1 (Supplementary Tables). Based on the mean monthly precipitation in Suriname, a year is divided into a wet season and a dry season.

There is a large intermodel spread for the CMIP models. Figure 8 (right) shows the monthly precipitation in mm/day for all models taken into account individually. The figure illustrates the large differences between models. Most models have a relatively low precipitation in comparison with the observations. There are a few models with a much higher mean precipitation.

The peak in monthly precipitation is in May for the observational datasets. However, for CMIP models the peak is in June. There seems to be a shift of one month in the progression of the monthly precipitation according to the CMIP historical projections in comparison to the observations.

In conclusion, the climatology of climate models is highly variable, the observed mean precipitation in Suriname is much higher (GPCP: 2020 mm/year, CRU: 2249 mm/year) than the historical mean CMIP precipitation projections (1428 mm/year) and there is a difference of one month in the highest monthly precipitation between observations and climate models.

### 4.2. Precipitation bias

The accuracy of projected precipitation by climate models is analysed by comparing the CMIP multimodel mean with the mean GPCP observations for the period 1991-2020. The comparison of spatial distribution of precipitation between models and observations indicates how well climate models can project intensity and position of precipitation events in Suriname and on a global scale.

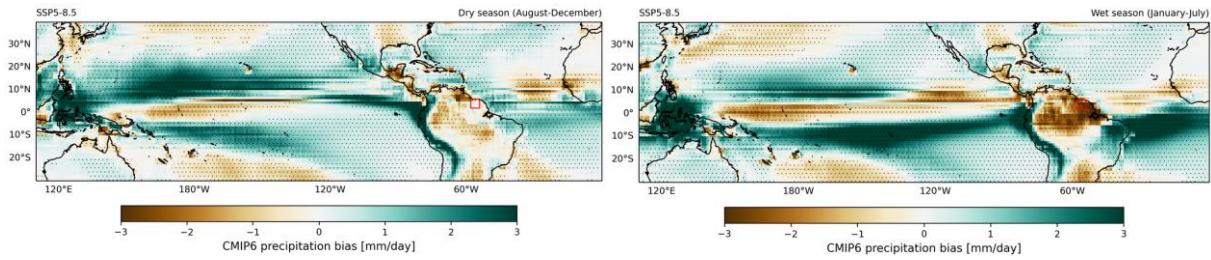


**Figure 9:** Mean CMIP precipitation bias (1991-2020) in the dry season (Aug-Dec) and the wet season (Jan-Jul), CMIP – GPCP in mm/day. Hashed regions have a significant multimodel mean at a 95% confidence level.

The dry season has a low relative and a low absolute precipitation bias in Suriname (Figure 9). The wet season has a strong negative bias. A double ITCZ bias in the Pacific and a dipole in the Atlantic are visible in the wet season. Here, climate models underestimate precipitation at the equator and overestimate precipitation south of the equator. This indicates that the historically simulated ITCZ has a lower mean latitude than the observed ITCZ. Figure 10 shows the mean CMIP precipitation bias in Suriname. Here, it is clearly pictured that there is a large difference between biases in dry and wet seasons.

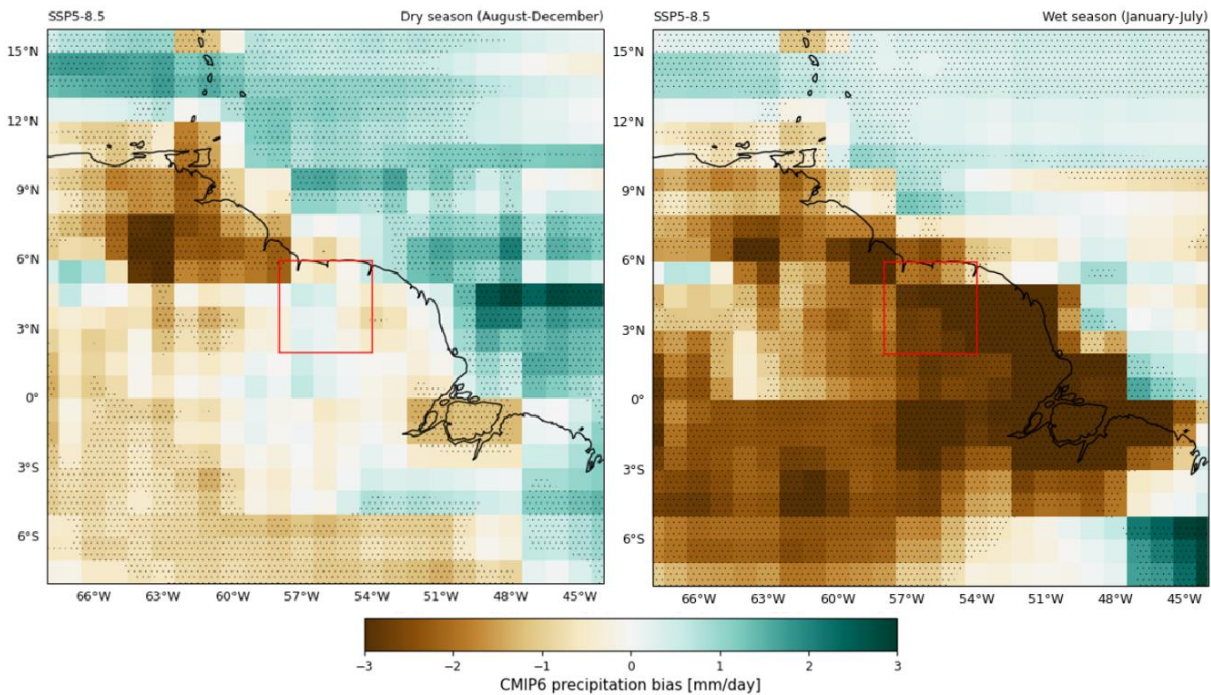


**Figure 10:** Zoomed spatial plot of mean CMIP precipitation bias (1991-2020) in the dry season (Aug-Dec) and the wet season (Jan-Jul), CMIP – GPCP in mm/day. Hashed regions are significant at a 95% confidence level. Suriname is indicated with the red square.

In Figure 11 the GPCP data and CMIP data for mean precipitation are placed next to each other to compare the location of the ITCZ in different months. The ITCZ above Suriname is simulated at a lower latitude on average by the CMIP models for every month in comparison to GPCP observations. This explains the different peak months (Figure 8) for precipitation between climate models and observations.

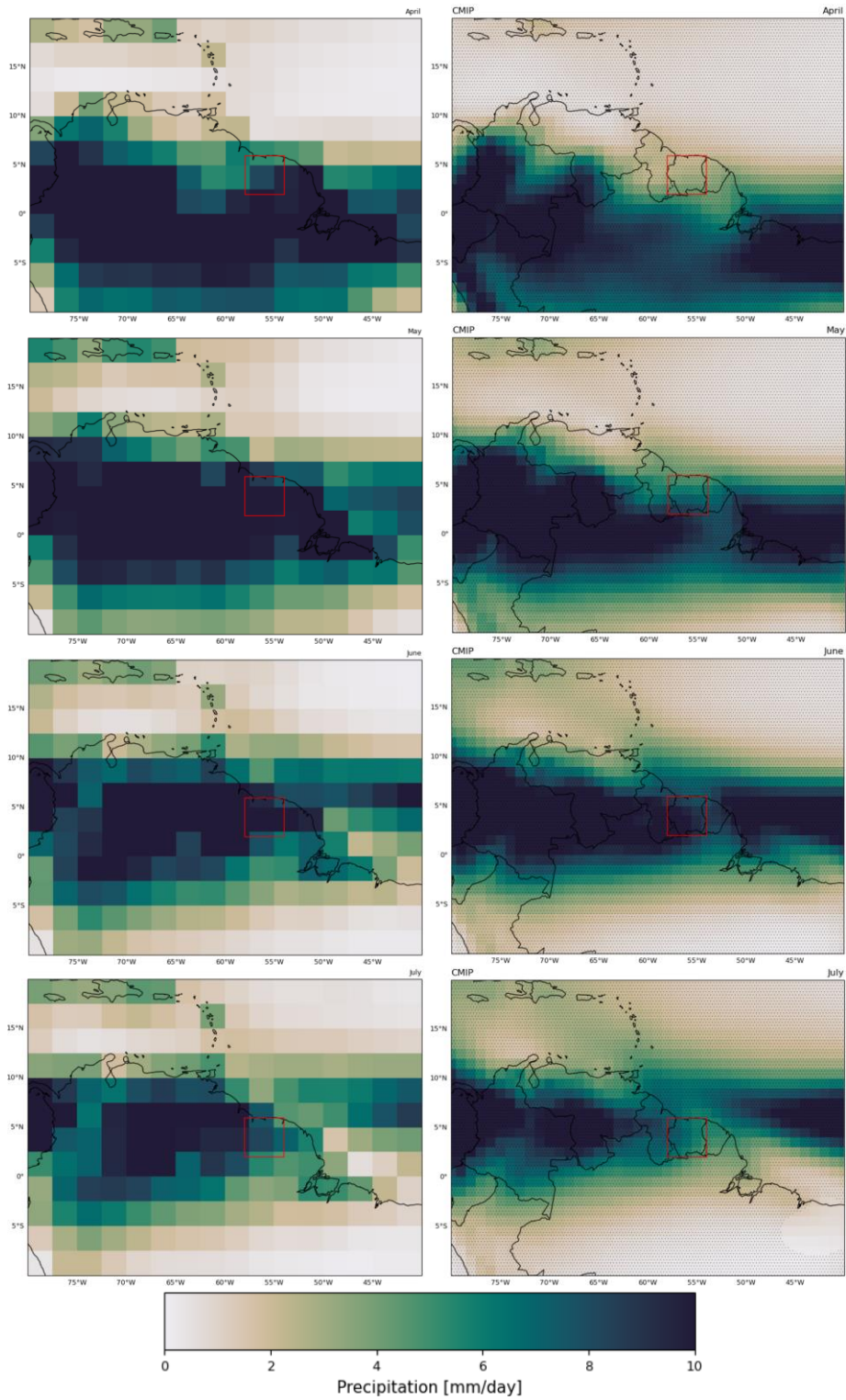


**Figure 11:** Monthly mean precipitation in mm/day from 1991 to 2020. On the left GPCP observations and on the right CMIP model mean. The red square indicates Suriname.

### 4.3. Climate drivers of Suriname

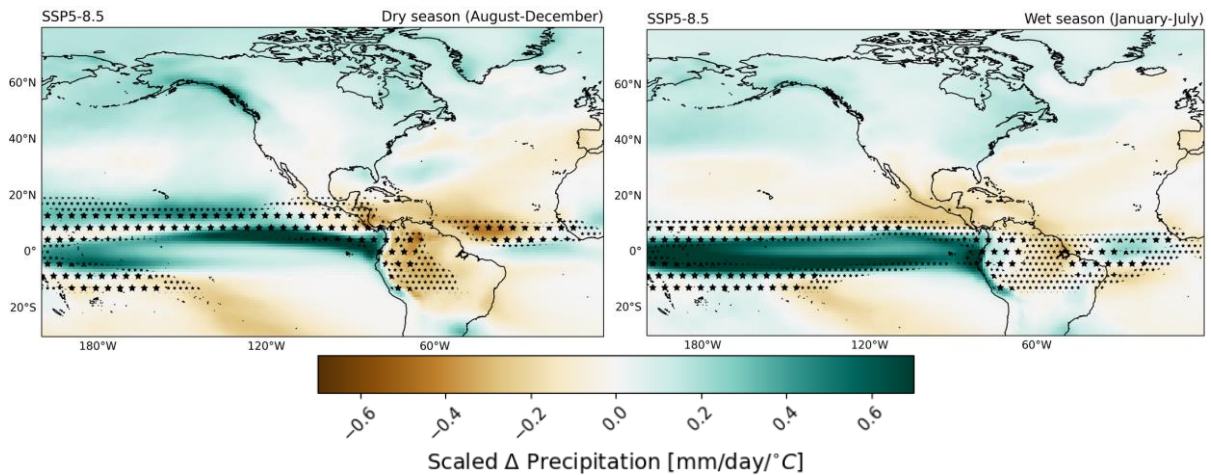


**Figure 12:** Scaled change in precipitation in mm/day/°C. 2085 (2071-2100) – 2005 (1991-2020). CMIP SSP5-8.5 scenario for the dry season (left) and the wet season (right). Precipitation scaled for mean temperature difference 2085 (2071-2100) - 2005 (1991-2020) in the area 40°S-40°N. Small and big stars are multimodel mean historical precipitation. Small stars indicate precipitation higher than 4 mm/day, big stars indicate precipitation higher than 6 mm/day.

A strong increase in precipitation in the Intertropical Convergence Zone (ITCZ) is projected in the Pacific Ocean for both seasons (Figure 12). The ITCZ above the tropical Atlantic Ocean has a weaker increase in precipitation than the Pacific ITCZ. Models project drying in the subtropical Atlantic Ocean. However, the mean precipitation change over Suriname is negative. Especially in the dry season, a decrease in precipitation in the tropics and subtropics is projected by the climate models.

The small and big stars in Figure 12 indicate the ITCZ simulated by the multimodel mean historical climate models. This indicated historical ITCZ gives the impression that the ITCZ is shifting to the south. The scaled change in precipitation is positive below the historical ITCZ in the Pacific for the dry and wet season, and positive below the historical ITCZ in the Atlantic in the dry season. In the wet season the scaled change in precipitation is positive in the upper part of the historical ITCZ in the Atlantic and in the dry season the scaled change in precipitation is positive in the upper part of the ITCZ in the Pacific and negative in the upper part of the historical ITCZ in the Atlantic.

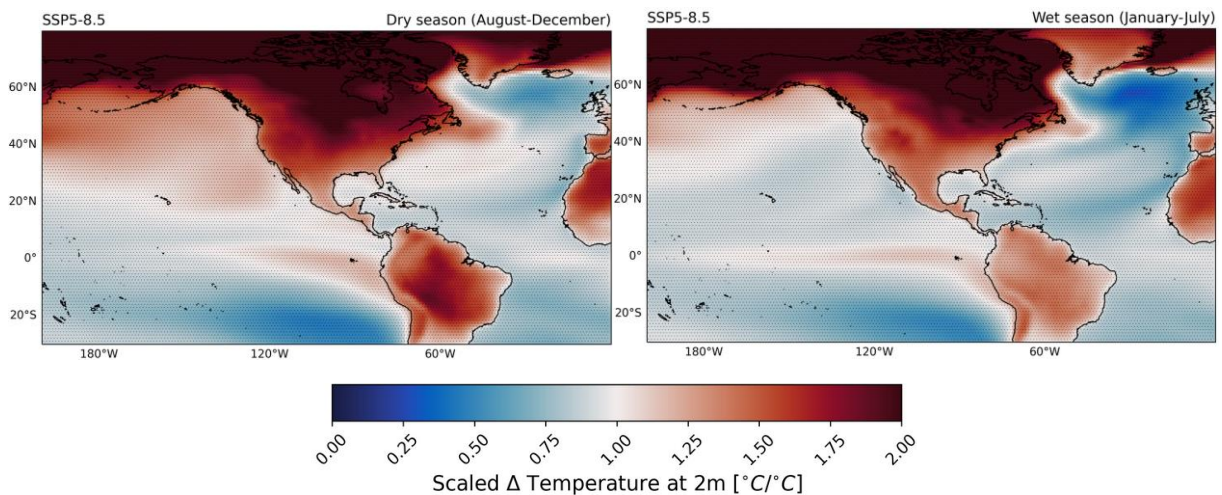


**Figure 13:** Scaled change in temperature at 2 m in °C/°C. 2085 (2071-2100) – 2005 (1991-2020). CMIP SSP5-8.5 scenario for the dry season (left) and the wet season (right). Temperature scaled for mean temperature difference 2085 (2071-2100) - 2005 (1991-2020) in the area 40°S-40°N.

Land area has a stronger warming than the oceans. Climate models also project a strong warming over the tropical East Pacific Ocean. In Figure 13 the multimodel mean scaled change in temperature at 2 m is shown for the dry season (left) and wet season (right). Values above one mean a stronger warming than the mean warming over the 40°S-40°N area.

A dipole is present in the north Atlantic Ocean. The northern subtropical Atlantic shows a relative strong warming compared to other Atlantic regions. The northern Atlantic ocean cools down and the region south of Greenland has a very strong temperature reduction.

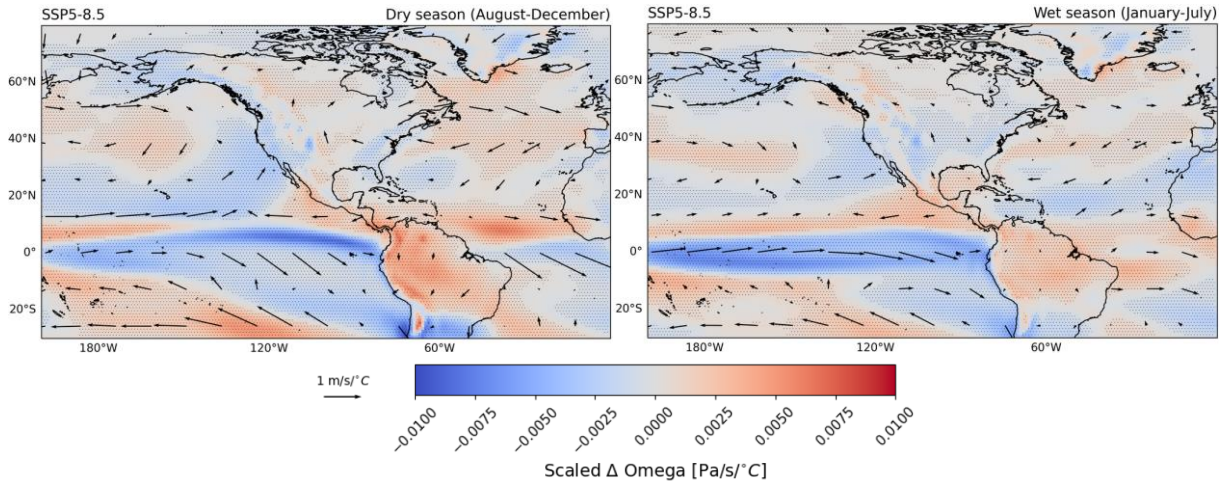


**Figure 14:** Scaled change in omega at 500 hPa in Pa/s/°C. 2085 (2071-2100) – 2005 (1991-2020). CMIP SSP5-8.5 scenario for the dry season (left) and the wet season (right). Wind at 850 hPa is also included with vectors in m/s/°C. Omega scaled for mean temperature difference 2085 (2071-2100) - 2005 (1991-2020) in the area 40°S-40°N. Omega is the vertical velocity in pressure coordinates where a positive value indicates an increase in downward vertical motion in the atmosphere.

Models project an increase in downward motion over Suriname (Figure 14). A downward motion results in a decrease in precipitation, which is also shown in Figure 12. Models project an increase in upward motion of air over the east Pacific ITCZ. Upward movement leads to an increase in deep convection and thus an increase in precipitation. Figure 12 shows that an increase in precipitation is present above the tropics in the east Pacific.

#### 4.4. Dry and wet models

First a division is made between models with historically high projected precipitation and models with historically low projected precipitation. The mean precipitation is taken from 1991 to 2020 for every model. Each group contains 10 models. The choice for 10 models is based on an even division between the amount of groups, since there are 31 models in total. There is a high difference in precipitation between these historically wet and dry groups (Figure 15). However, both the historically wet and historically dry group project on average a decline in annual precipitation for Suriname. The absolute decrease in precipitation is similar for the historically wet and historically dry group. Therefore the decrease in absolute precipitation does not seem to depend on historical precipitation intensity.

The precipitation bias in the climatology of the historical climate projections does not explain the differences between model projections, because the absolute change in precipitation does not depend on historical precipitation. That is why another approach is made to get an explanation for the different model projections of precipitation, and thus an explanation for the intermodel spread.

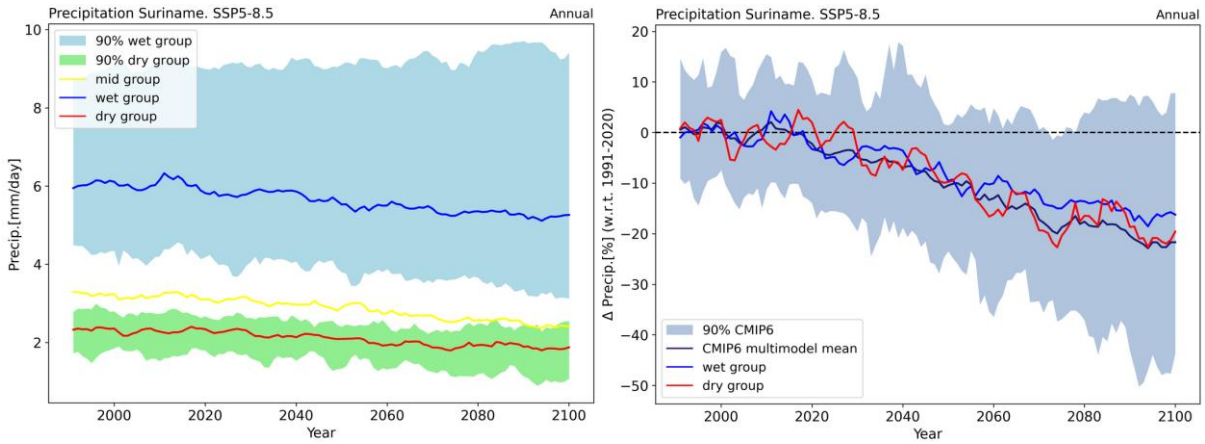


**Figure 15:** Historically wet and dry groups. Absolute precipitation (left) and the percentage change in precipitation (right).

In the next approach, separate groups of wet and dry models are made, with a dry model defined as a model with a large decrease in precipitation and a wet model with a low decrease in precipitation or an increase in precipitation. The reason for defining the different groups of models this way is because this will give insights on the large intermodel spread for precipitation change. This is done by looking at the difference in mean precipitation from period 2071-2100 and mean precipitation in period 1991-2020 in Suriname, scaled by the mean temperature difference projected from period 2071-2100 and period 1991-2020 by the model over the area 40°S-40°N.

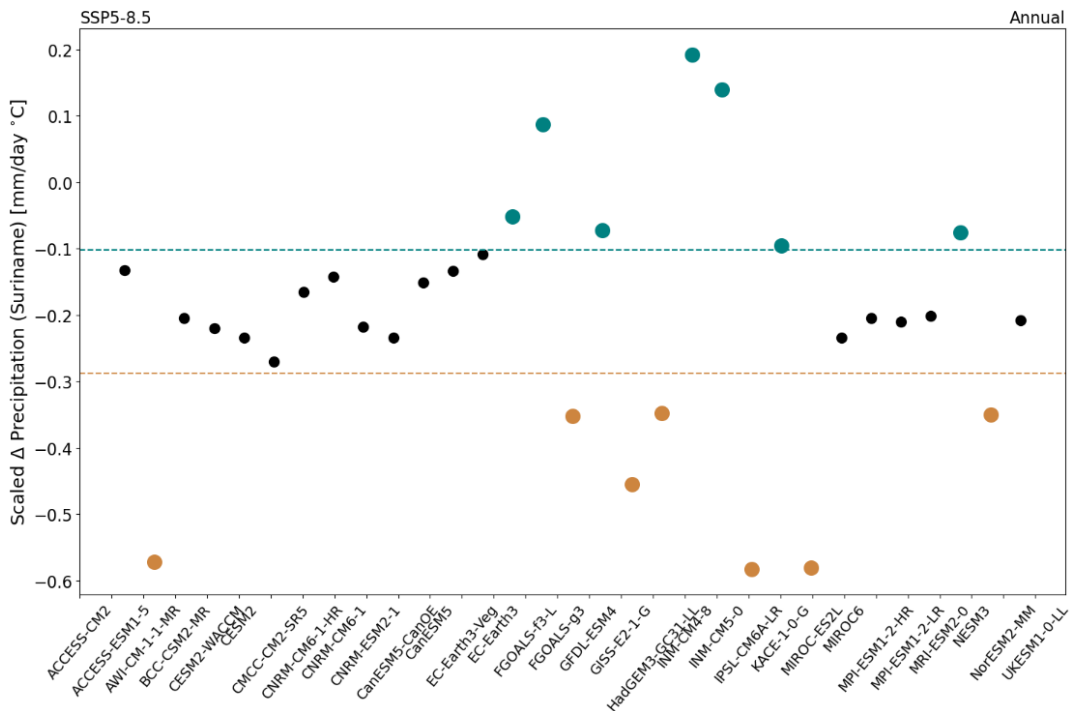


**Figure 16:** The scaled change in precipitation for every climate model. Mean precipitation difference in mm/day for 2085 (2071-2100) - 2005 (1991-2020) in Suriname, scaled for mean temperature difference 2085 (2071-2100) - 2005 (1991-2020) in the area 40°S-40°N. Colors indicate which group a model is assigned to.

In Figure 16 the scaled change in precipitation is given for every model. Here, the models are assigned to a group based on an almost equal distribution of scaled change in precipitation divided

into three parts, being the dry, middle and wet group. In this way, models projecting precipitation close to the multimodel mean precipitation projection are in the middle group. As a result seven models have been assigned to the dry group, seven to the wet group and the remaining 17 models constitute the middle group. Only three climate models have a projected increase in precipitation.

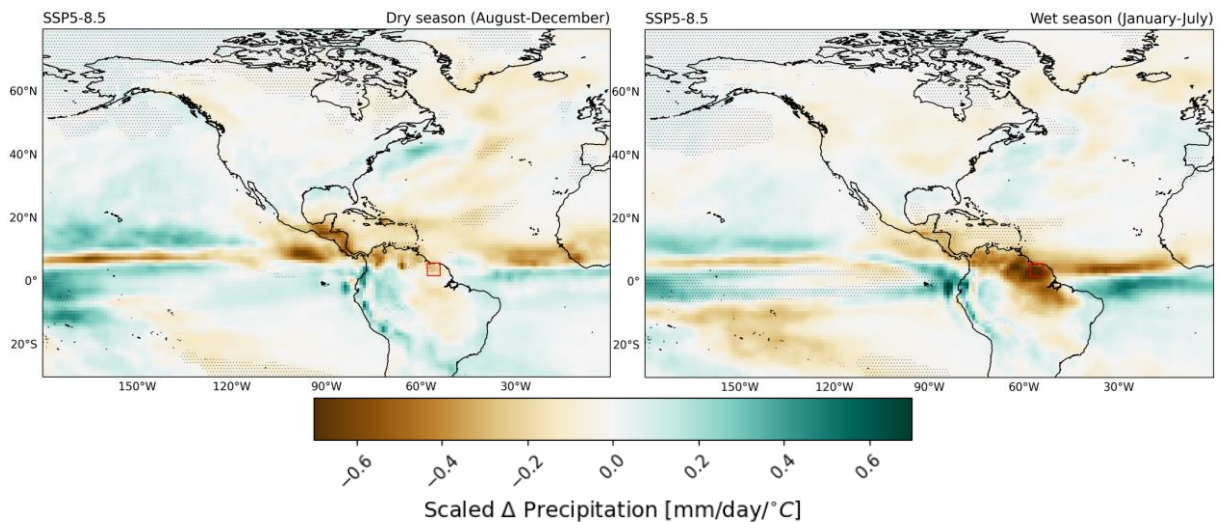


**Figure 17:** The difference in scaled change in precipitation between dry and wet models in mm/day/°C. The multimodel mean for the dry group – multimodel mean for the wet group is taken for the change in precipitation between 2085 (2071-2100) and 2005 (1991-2020). A negative value on the figure indicates that dry models project more drying than the wet models. Dry season (left) and wet season (right). Hashed regions are significant at a 95% confidence level. Suriname is indicated with the red square.

In the wet season, models from the dry group project much stronger drying in Suriname than models from the wet group, a difference of more than 0.6 mm/day per degree warming (Figure 17). There is little difference in drying in Suriname between the wet and dry group in the dry season. Most regions in Figure 17 have a negative value because the dry group projects larger drying than the wet group by definition. However, there are also regions with positive values. These positive regions, mostly occurring below the equator, are regions where the CMIP multimodel mean projects an increase in precipitation (Figure 12). This means dry models project a stronger increase in precipitation than wet models in these regions.

In the wet season, a dipole in precipitation is present above the tropical Atlantic Ocean where the ITCZ is located. The dipole in precipitation follows from a stronger decrease in precipitation above the equator and a stronger increase in precipitation below the equator, for the dry group in comparison to the wet group.

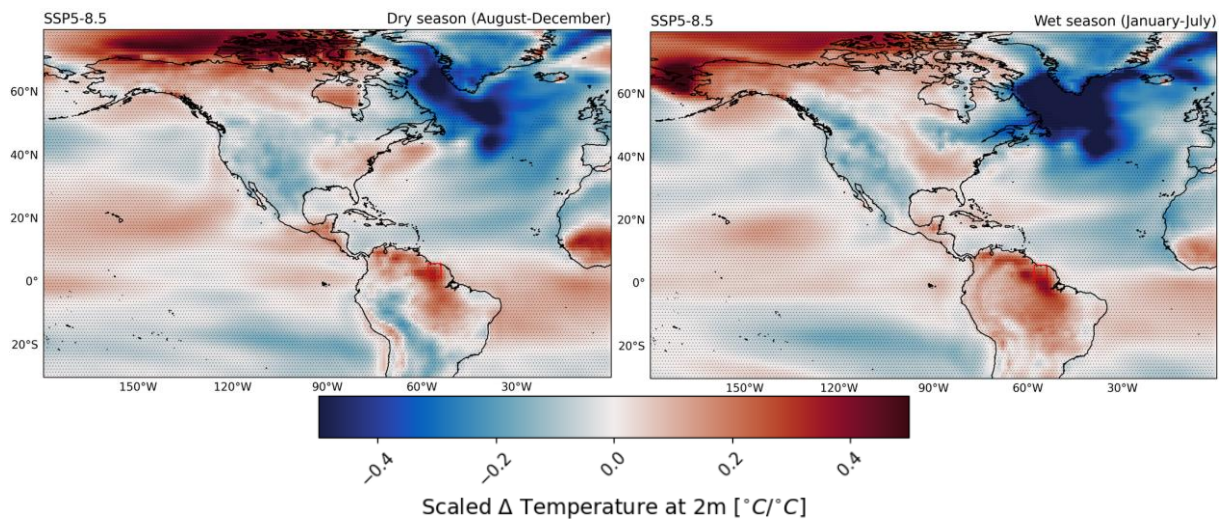


**Figure 18:** The difference in scaled change in temperature between dry and wet models in  $^{\circ}\text{C}/^{\circ}\text{C}$ . A positive value on the figure indicates dry models projecting a higher mean temperature than wet models. Dry season (left) and wet season (right). Hashed regions are significant at a 95% confidence level. Suriname is indicated with the red square.

A temperature dipole is present above the tropical Atlantic Ocean (Figure 18) just like the precipitation dipole in Figure 17. Dry models project more warming in Suriname and below the equator. The Northern Atlantic ocean cools down and the region south of Greenland has a very strong scaled temperature reduction for dry models in comparison to wet models.

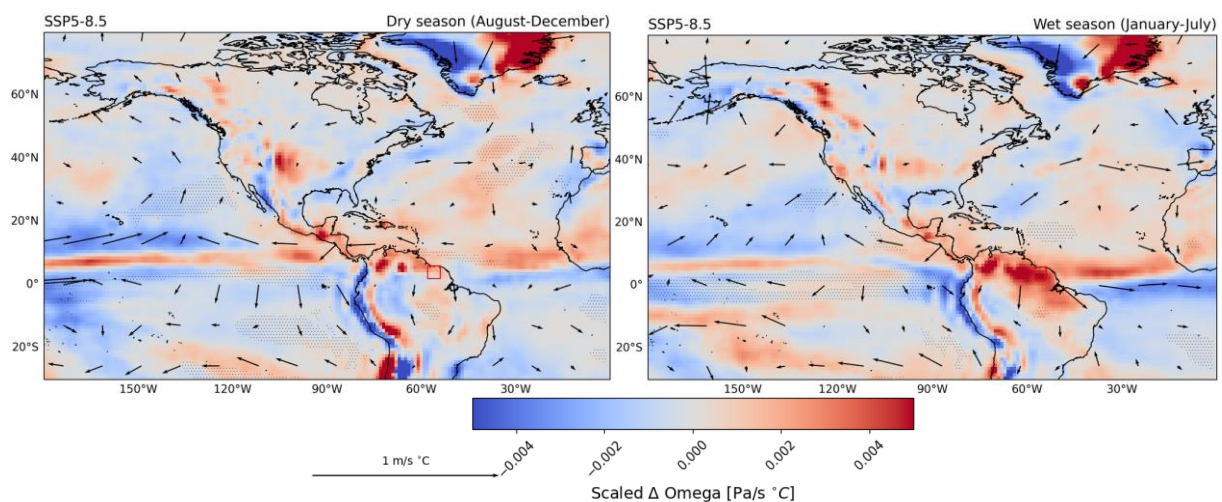


**Figure 19:** The difference in scaled change in omega between dry and wet models in  $\text{Pa/s}/^{\circ}\text{C}$ . Dry season (left) and wet season (right). Wind at 850 hPa is also included with vectors in  $\text{m/s}/^{\circ}\text{C}$ . The vectors indicate magnitude and direction of wind at 850 hPa. Negative values indicates a stronger upward air movement for dry models. Hashed regions are significant at a 95% confidence level. Suriname is indicated with the red square.

Dry models project a higher decrease in precipitation than wet models. Fewer clouds will be present above Suriname with less precipitation. Both wet and dry season indicate a stronger upward air movement for dry models in the Pacific Ocean at the west coast of South-America. The wet season shows strong downward movements above Suriname (Figure 19). This also explains the higher temperatures for dry models (Figure 18) because it is warmer during the day when there are no clouds over the land.



## 4.5. April & May

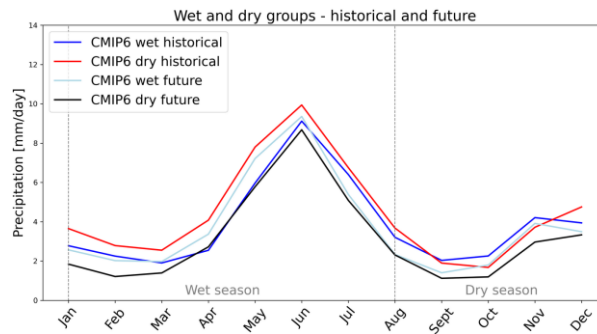


**Fig 20:** Monthly precipitation for Suriname in mm/day for CMIP wet group historical mean (1991-2020), CMIP dry group historical mean (1991-2020), CMIP wet group SSP5-8.5 mean (2071-2100) and CMIP dry group SSP5-8.5 mean (2071-2100).

The months April and May are interesting because these are the only two months showing an increase in precipitation (Figure 20). The dry group is drier in the future in all months. Analysing these months through a comparison with two other months (July & August) where the dry and wet group have a similar change in precipitation, can give insights on the different behaviours of the climate models.

Again, projections have been made for scaled temperature, scaled precipitation and scaled omega, but now for the mean of the months April & May and for the mean of the months July & August. Figure S.3 and Figure S.4 (Supplementary Figures) show the mean scaled change in precipitation, mean scaled change in temperature and mean scaled change in omega at 500 hPa (with wind vectors at 850 hPa) in April & May (left) and July & August (right) for the dry models and the wet models respectively.

### April & May

For both the dry and wet models there is a warming of the tropical Atlantic Ocean. This is a source of enhanced precipitation. However, for the dry models there is also an increased warming south of the equator and a reduced warming north of the equator.

Due to the tropical Atlantic warming, there is an increase in precipitation along the equator in the Atlantic in the wet models. A decrease in precipitation is visible south of the equator in the Atlantic Ocean.

### July & August

Wet models project an increase in precipitation in the eastern part of the tropical Atlantic Ocean. The dry area over Suriname extends to the Caribbean and Central America.

Along the equator there is an Atlantic Niño in the Atlantic Ocean that extends from the African coast to about halfway up the Atlantic Ocean. The mechanism of the Atlantic Niño is the same as the El-Niño on the Pacific Ocean. This pattern is also visible in warming in climate models, just like in the Pacific Ocean.

#### 4.6. Atlantic Meridional Overturning Circulation (AMOC)

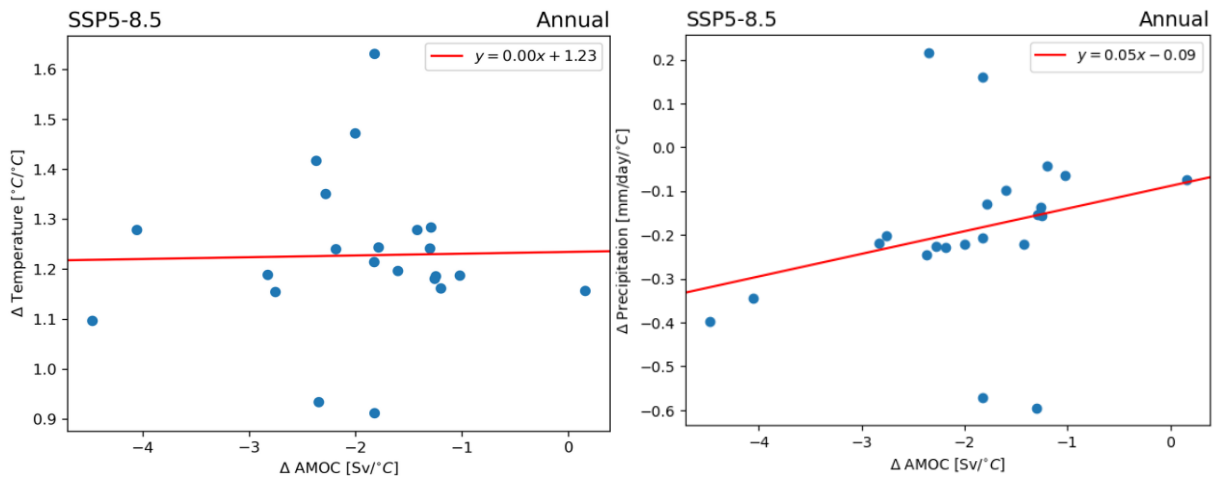


**Figure 21:** scatterplots of correlation: Scaled change in temperature [ $^{\circ}\text{C}/^{\circ}\text{C}$ ] vs scaled change in AMOC [ $\text{Sv}/^{\circ}\text{C}$ ] (left) and scaled change in precipitation [ $\text{mm}/\text{day}/^{\circ}\text{C}$ ] vs scaled change in AMOC [ $\text{Sv}/^{\circ}\text{C}$ ] (right). 2085 (2071-2100) – 2005 (1991-2020). 21 models are used.

There is no correlation between change in scaled AMOC strength and change in scaled temperature (Figure 21). However a positive correlation exists between scaled change in precipitation and scaled change in AMOC strength, with a Pearson correlation coefficient of  $r = 0.22$ . The Pearson correlation is not significant, but there is a visible correlation. 19 out of the 22 models project both a decrease in precipitation and a decrease in AMOC strength.

#### 4.7. Coast and inland

Figure S.5 (Supplementary Figures) implies that there are differences in historical precipitation in Suriname between the coast and inland of Suriname for both CMIP and CRU. CRU is used here because it has a higher resolution than GPCP. The coast of Suriname has a higher precipitation in the dry season than the inland of Suriname, whereas the inland has a higher precipitation in the wet season than the coast. The main reason that the coast has a higher rainfall in the dry season and the inland a higher rainfall in the wet season is the movement of the ITCZ. The projected change in precipitation seems to progress in a similar pattern and magnitude for all three analysed regions.

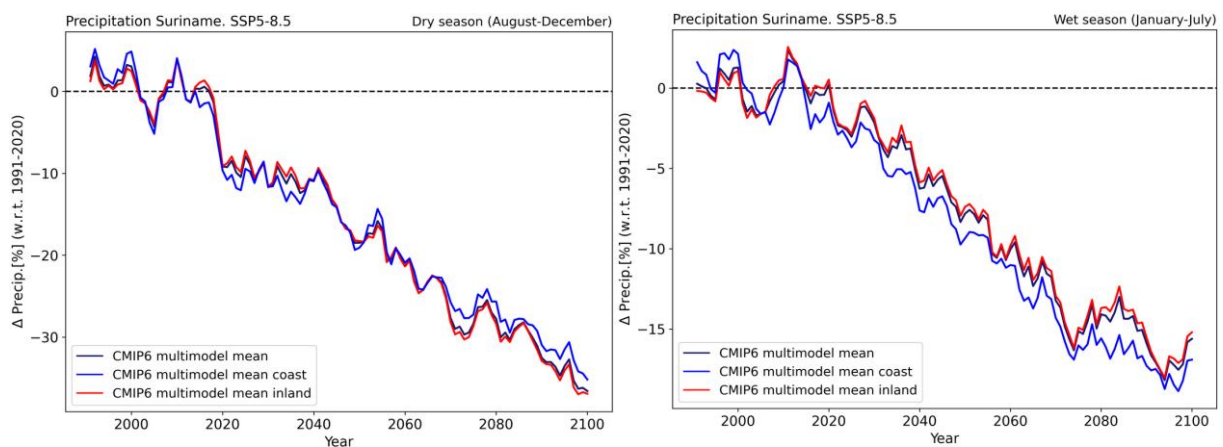


**Figure 22:** Percentage change in precipitation time series for CMIP. Suriname, coastland of Suriname and inland of Suriname. Precipitation change in % with regard to the multimodel mean of the period 1991-2020. The

longitude interval chosen is  $[302^\circ - 306^\circ]$  for every region. The latitude for the regions are: Suriname  $[2^\circ - 6^\circ]$ , the coast  $[5^\circ - 6^\circ]$  and the land  $[2^\circ - 5^\circ]$ .

As can be seen from Figure 22 and Figure S.6 (Supplementary Figures) the climate models project similar patterns in precipitation change between the coast and inland of Suriname. There are two potential reasons for this occurrence. The first cause can be that there are not much differences in precipitation change between these regions. Another reason could be the low resolution for some climate models. When a climate model has a low resolution the model may not be able to project different changes in climate between adjacent regions, even when these regions have differences in climate in historical climate simulations.

#### 4.8. Quantile Delta Mapping

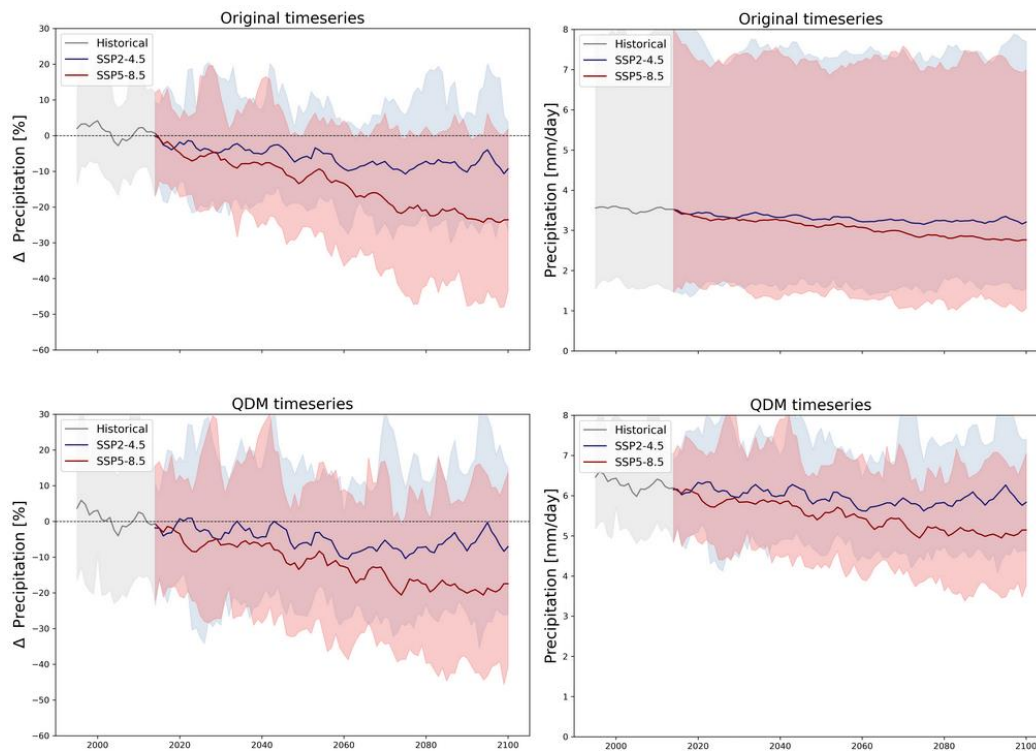


**Figure 23:** CMIP multimodel change in annual precipitation for Paramaribo relative to 1991-2020 average, for the SSP2-4.5 and SSP5-8.5 scenarios. The shaded area is the 90% intermodel spread. Left figures show the relative changes and right figures show the absolute changes.

The intermodel spread in precipitation projections by climate models has become smaller after the QDM correction (Figure 23, right). The 90% intermodel spread changed from 1-8 mm/day to 4-7.5 mm/day. Next to that, QDM correction has shifted the historical multimodel mean precipitation upwards by approximately 3 mm/day, almost doubling it. Another difference between original and QDM time series is the higher variability in the QDM timeseries.

The multimodel mean relative changes in precipitation are nearly equal for the original and QDM corrected models (Figure 23, left), as is expected due to climate sensitivity of the models remaining unaffected.

Models project higher precipitation decrease in Paramaribo for scenarios SSP5-8.5 compared to scenario SSP2-4.5. This does not change when the models are corrected by QDM. Both scenarios have about the same variability, which does not differ much after the QDM correction. In addition,

the intermodel spreads of the scenarios do not seem to differ much from each other, for both the absolute and the relative values.

Historical and future CDFs for precipitation from original climate models are similar (Figure 24, top). They both have a large spread in CDFs for the models ranging from models with a lot of low values (lower than 5 mm/day) to models with very few low values. According to the Cultuurtuin observations there is no precipitation for more than 40% of the days, whereas climate models all have no precipitation in less than 10% of all days, with many values below 1 mm/day. All original climate models have few precipitation values above 10 mm/day in comparison to the Cultuurtuin. All CDFs for QDM historical models resemble the Cultuurtuin CDF, as is expected because the CDF is incorporated and adjusted for the projection period on the basis of the difference between the model and observational CDFs. Future QDM CDFs still follow the same trend as Cultuurtuin but most models tend to have more values lower than 10 mm/day and more values higher than 50 mm/day in comparison to Cultuurtuin.

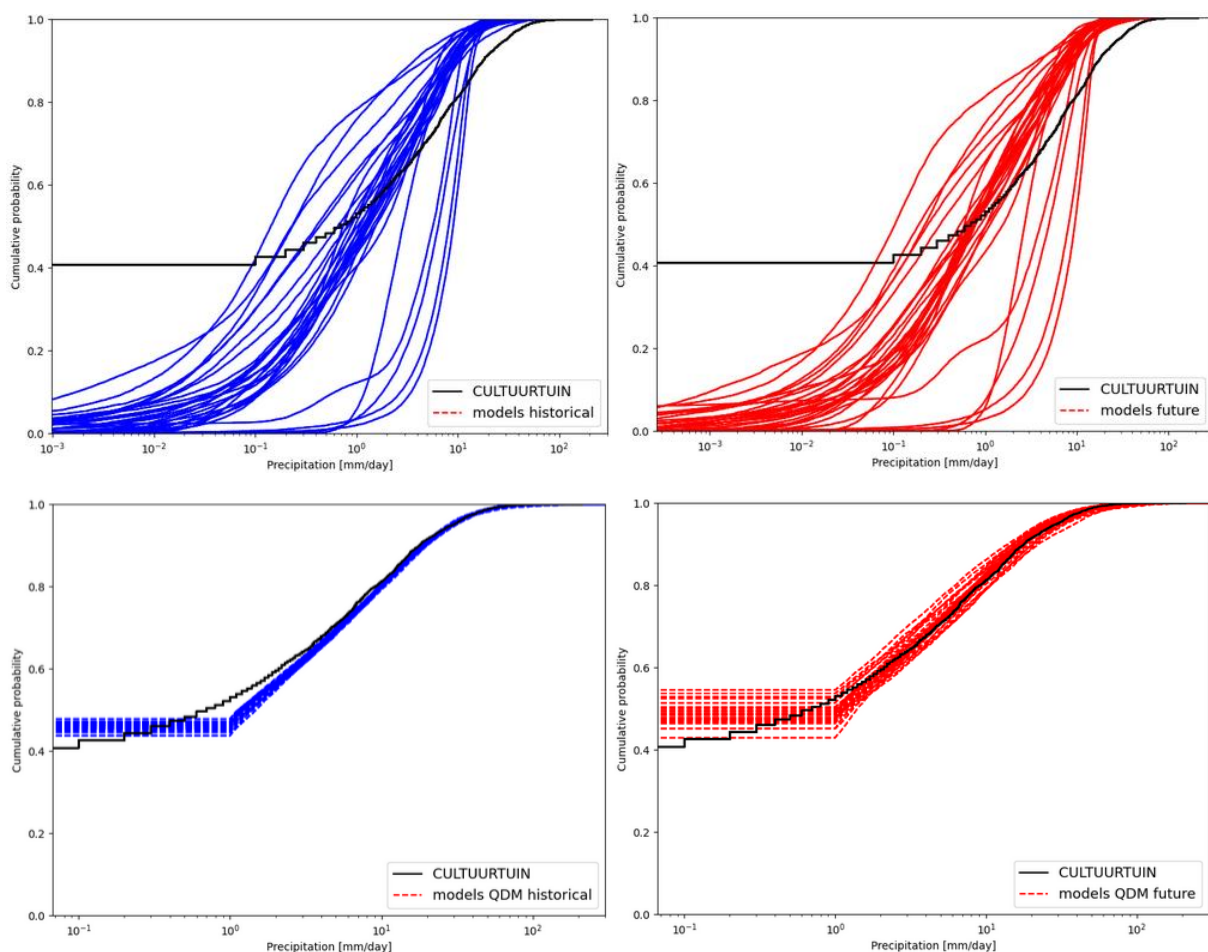


**Figure 24:** CMIP model precipitation CDFs for historical (top left), future (top right), QDM historical (bottom left) and QDM future (bottom right) for SSP2-4.5. Daily values from 1991-2020 for historical and daily values from 2071-2100 for future, for Paramaribo. The x-axis has a logarithmic scale.

## 4.9. Extreme precipitation

### One-day extremes

The 10% extreme precipitation decreases for every season, model group and scenario (Table 1 and B.2). This almost also applies to the 5% extreme precipitation. Here only wet models for scenario SSP5-8.5 do not project a decrease.

The highest extremes, 0.1% extremes, increase annual and in the wet season for all model groups. The increase of 0.1% extremes is relatively high compared to changes of the other extremes, with the highest increased values for scenario SSP5-8.5.

Dry models have less extreme values in the future for all extremes except 0.1%. Both the decreases in the lower extremes and the increases in the higher extremes are higher for SSP5-8.5 than SSP2-4.5 for the dry models. Wet models project low decreases and high increases for every extreme percentages in comparison to other models.

	season:	annual				dry season				wet season			
	percentage extremes:	10%	5%	1%	0.1%	10%	5%	1%	0.1%	10%	5%	1%	0.1%
all models	relative change (%)	-21.67	-15.40	-2.47	12.65	-25.45	-21.14	-10.82	-4.93	-19.33	-11.32	-0.25	14.90
	absolute change (mm/day)	-4.14	-4.53	-1.50	8.72	-3.65	-4.90	-5.10	-6.93	-4.30	-3.77	-0.24	11.94
dry models	relative change (%)	-32.39	-25.25	-13.18	19.22	-31.03	-27.07	-18.01	-9.47	-31.79	-23.53	-9.00	19.96
	absolute change (mm/day)	-6.14	-7.35	-7.20	16.50	-4.43	-6.16	-8.08	-6.84	-6.96	-7.69	-5.42	18.44
wet models	relative change (%)	-6.44	0.16	15.68	25.29	-24.26	-15.33	-3.64	1.97	-0.08	9.95	16.17	25.10
	absolute change (mm/day)	-1.25	-0.01	8.59	24.82	-3.58	-3.52	-1.59	1.14	-0.11	3.16	10.04	28.17

**Table 1:** one-day cumulative extreme precipitation for SSP5-8.5. The values represent the mean of the change in extremes of the models, 2085 (2071-2100) – 2005 (1991-2020). 28 models in all models, seven dry models and seven wet models.

### Five-day cumulative extremes

The five-day cumulative extremes changes are similar to the one-day extremes changes (Table 2 and B.3). The 10% extreme is decreasing in every case except for wet models in the wet season and the 0.1% extremes increase except for in the dry season.

Again, the dry models project a decrease in extreme precipitation for all extremes except the 0.1%. Wet models have more increasing precipitation extremes in comparison to other models.

	season:	annual				dry season				wet season			
	percentage extremes:	10%	5%	1%	0.1%	10%	5%	1%	0.1%	10%	5%	1%	0.1%
all models	relative change (%)	-16.56	-9.48	2.13	10.87	-22.70	-18.95	-11.21	-10.71	-12.39	-4.49	4.91	15.78
	absolute change (mm/day)	-13.56	-10.84	2.49	20.53	-13.91	-16.65	-17.99	-42.39	-11.79	-5.84	8.07	35.45
dry models	relative change (%)	-25.65	-18.89	-5.78	12.03	-28.41	-24.32	-17.09	-12.52	-23.18	-14.67	-2.13	10.67
	absolute change (mm/day)	-20.73	-20.61	-10.74	24.63	-17.19	-20.60	-23.47	-28.38	-21.74	-18.25	-5.73	18.57
wet models	relative change (%)	-0.72	9.80	23.21	28.41	-17.62	-10.57	3.92	-7.63	7.27	17.65	25.23	35.62
	absolute change (mm/day)	-0.77	10.31	41.89	85.56	-10.57	-9.18	4.92	-15.02	6.52	21.67	51.22	111.35

**Table 2:** five-day cumulative extreme precipitation for SSP5-8.5. The values represent the mean of the change in extremes of the models, 2085 (2071-2100) – 2005 (1991-2020). 28 models in all models, seven dry models and 7 wet models.

## 5. Discussion

As already stated in the method section, most results are only given for emission scenario SSP5-8.5, because temperature and precipitation patterns in CMIP models only slightly change under increasing or decreasing concentrations of greenhouse gases. The changes in precipitation, temperature and omega scaled for temperature are similar for scenarios SSP2-4.5 and SSP5-8.5. Therefore, the focus on the analyses of scenario SSP5-8.5 does not influence the conclusions.

### **Climate drivers of Suriname**

The strong increase in precipitation in the ITCZ projected by climate models in the Pacific Ocean indicates a strengthening of deep convection over the Pacific tropics. Sea surface temperature warming in the tropical eastern Pacific plays an important role for the increase in precipitation (Sun et al., 2020).

Stronger warming over land is a consequence of lapse-rate changes associated with tropospheric moisture contrasts. The relative humidity is higher above the oceans than over land areas (Brogli et al., 2019). Also, the North Pole has a strong warming compared to other land areas. This is caused by a phenomenon known as polar amplification. Changes in the net radiation balance have a greater impact on the change in temperature near the poles than the global average temperature change. Theories suggest the ice-albedo feedback, water vapour feedback, lapse rate feedback and ocean heat transport as possible causes (Lee, 2014).

Stronger warming over the tropical east Pacific indicates a stronger El Niño Southern Oscillation (ENSO) effect. Climate models project more El Niño like conditions in the future under global warming (Bayr, 2013). Consequences are a weakening of the mean zonal circulation along the equator and an eastward migration of the Walker circulation in the Pacific. In contrast to the simulated weakening and eastward migration of the Walker circulation by models, observations from the past 50 years show a strengthening of the Walker circulation, related to a westward migration of the Walker circulation or La Niña like conditions (Brotons et al., 2023). This is an issue that has already been reported in previous CMIP versions (Seager et al., 2019) and CMIP6 (Wills et al., 2022) but still requires further investigation.

The northern Atlantic Ocean cooling down and strong temperature reduction in the region south of Greenland is probably caused by the weakening of the Atlantic Meridional Overturning Circulation (AMOC) (Zhang, 2010). With the weakening of the AMOC less warmth is being transported from the south Atlantic Ocean to the north Atlantic Ocean, enhancing the warming of the south Atlantic Ocean and cooling of the north Atlantic Ocean. A weakened AMOC leads to a southward shift of the ITCZ in the Atlantic Oceans.

The occurrence of an increase in upward motion over the Pacific ITCZ and an increase in downward motion over Suriname indicate an eastward migration of the Walker Circulation. With an eastward migrated Walker circulation an upward motion of moisture is strengthened in the Pacific ITCZ and deep convection is increased (Sun et al., 2020). Another reason for an increase in precipitation in the Pacific ITCZ is the positive feedback between convection and cloud radiative forcing. Under global warming the amount of clouds increases due to enhanced deep convection which then strengthens deep convection by increasing longwave heating into the atmosphere (Sun et al., 2020).

## Dry and wet Models

The dipole in precipitation above the tropical Atlantic Ocean, with a decrease in precipitation above the equator and an increase in precipitation below the equator, implies that dry models project an enhanced southward shift in the ITCZ location compared to projections for wet models.

The northern Atlantic cooling down and the very strong temperature reduction for dry models in comparison to wet models in the region south of Greenland are probably caused by the different magnitudes of weakening of the Atlantic Meridional Overturning Circulation (AMOC) between the different groups of models. As the weakening of the AMOC results in less warmth being transported from the south Atlantic Ocean to the north Atlantic Ocean, consequently leading to warming of the south Atlantic Ocean and cooling of the north Atlantic Ocean, the ITCZ shifts southward. When the location of the ITCZ on average is more southward throughout the year, the ITCZ will be present over Suriname fewer days. This leads to a decrease in precipitation over Suriname for models projecting a southward shift of the ITCZ.

The choice to allocate seven models to the wet and dry groups of models did not have a major impact on the resulting results. If the same experiments are performed for 10 models per group, the results are almost identical. In contrast, the results are inexplicable in some regions if three extreme models are assigned per group. The results for the same experiments with three models in the dry group and three models in the wet group are shown in Figure S.7 (Supplementary Figures). Most patterns for seven models per group and three models per group are similar with stronger amplitudes for three models per group. The most remarkable difference between Figure 16 and Figure S.6 is that although they both have a polar amplification in the sub polar gyre south of Greenland, this sub polar gyre has more warming in the dry models compared to wet models for three models per group, while it has less warming in the dry models compared to wet models for seven models per group. Possible explanations for the results in Figure S.6 could be model errors, such as errors in the land-ocean system, parametrization errors, errors in simulating dynamical and atmospheric processes, etc.

### *April & May*

A precipitation decrease for wet models south of the equator in the Atlantic is probably caused by the ITCZ being south of the equator in historical projections by climate models. The tropical Atlantic warming moves the ITCZ towards the equator and causes the precipitation dipole. In the dry models, the effect of the stronger warming south of the equator dominates, which pulls the ITCZ to the south and makes the equator and Suriname drier.

### *July & August*

The precipitation increase in the eastern part of the tropical Atlantic is probably due to the stronger El-Niño signal, especially in the Niño 1,2 area, the area at the northern coast of South America (0°S-10°S, 80°W-90°W).

North of the equator in the Atlantic Ocean there is an inter-annual variation in sea surface temperature (SST) called the hemisphere or gradient mode (Vauclair and Du Penhoat, 2001). The main cause is the variation in the trade winds over that area. A weakening of this variation causes a reduction in evaporation from the sea surface and therefore warming. Strong anomalous westerly

winds over the tropical north Atlantic Ocean will appear during July & August, for both dry and wet models. This weakens the climatic northeast trade wind and results in warming. These anomalous westerly winds could be related to the El Niño signal on the Pacific Ocean. This causes descending air movement, through changes in the Walker Cell, over the Caribbean, Central America, the Pacific and northern South America. Its outflow causes the anomalous westerly winds across the Atlantic Ocean.

In summary, the mean position of the ITCZ is further north in the future for wet model projections in the months April & May compared to historical simulations, leading to a higher precipitation in Suriname. This does not happen in the months July & August. As opposed to wet models, dry model projections have a decrease in precipitation because of the dominating warming effect south of the equator, pulling the ITCZ more south and making Suriname drier than in the wet model projections.

## **AMOC**

The correlation between scaled change in AMOC strength and scaled change in precipitation suggests that the decrease in AMOC strength has an influence on the decrease in precipitation in Suriname. However, with the correlation not being significant, this influence cannot be determined with certainty.

The four outliers in Figure 21 (right), the two models with the highest increase in temperature and the two models with the highest decrease in precipitation, are noteworthy. These are the only four models far from the mean model trend in scaled change in precipitation vs scaled change in AMOC strength. In Figure S.8 (Supplementary Figures) the differences in scaled change in temperature, scaled change in precipitation and scaled change in omega between the two highest decrease in precipitation outliers and the two highest increase in precipitation outliers, for the dry season (left) and the wet season (right) are shown. The figures do not give explicable results. Neither the difference in changed temperature nor the difference in changed precipitation have realistic dynamical spatial patterns in some parts, like the subpolar gyre in the northern Atlantic Ocean south of Greenland. This leaves an uncertainty in the influence of the AMOC on the amount of precipitation in Suriname.

## **QDM**

The narrowing of the 90% intermodel spread for the multimodel mean annual precipitation after QDM correction can be considered a good improvement. In addition to the large original intermodel spread, the doubling of the multimodel mean precipitation indicates that climate models are incapable of accurately projecting precipitation in Paramaribo.

The choice was made to bias-correct climate models with QDM only for Paramaribo. Unfortunately, there was no time in this study to apply QDM and analyse the results for the whole of Suriname. Future studies could focus on QDM for the whole of Suriname, with QDM being applied to the climate models for as many grid points as possible. The local impact of uniform large-scale changes can be analysed for these grid points. In the chapter coast and inland it became clear that there are no major differences in climate projections of precipitation trends between the coast and the inland of Suriname, probably caused by the too coarse resolution of the climate models. Dynamical downscaling is necessary in order to investigate whether there are actual differences in precipitation trends in the future, between the coast and the inland of Suriname.



QDM has improved the cumulative distribution of precipitation for climate models. The distribution of the amount of precipitation in Paramaribo is completely different from observations for all climate models and this is corrected properly.

Cultuurtuin, CHIRPS and CHIRPS regridded have similar CDFs and ERA5 has a different CDF (Figure 25). The main reason for the different CDF for ERA5 is that this dataset has very few zero values. Precipitation values in ERA5 are calculated by a model. Models tend to have fewer zero values than observations. The ERA5 CDF starts at slightly higher than zero cumulative probability, whereas the CDFs for the other datasets start at higher than 0.4 cumulative probability. The fact that Cultuurtuin and CHIRPS have similar CDFs and that the extreme values of the CDFs are all approximately equal is positive with regard to the reliability of the values.

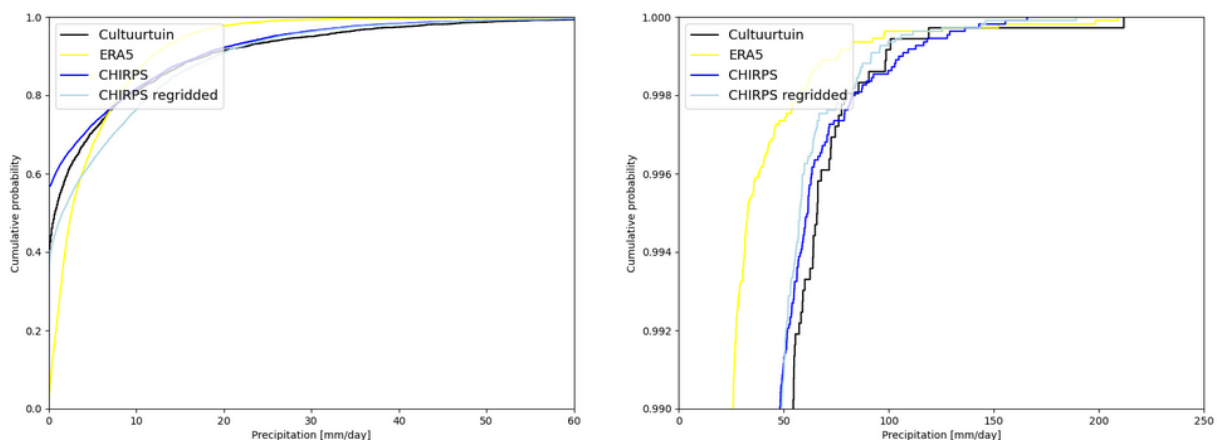


**Figure 25:** Precipitation CDFs for four different observational datasets with daily values from 1991-2020 in Paramaribo. Cultuurtuin has point observations and ERA5 and CHIRPS are gridded datasets.

An argument that could be made against using the Cultuurtuin dataset as a reference for QDM transformation is that Cultuurtuin has point observations, while the CMIP models have a resolution of 1 x 1 degrees. To analyse this argument, the gridded dataset CHIRPS has been regridded to a resolution of 1° x 1° and compared with Cultuurtuin and CHIRPS original (0.05° x 0.05°). As a result of the regridding to a lower resolution the CHIRPS regridded now has fewer zero values than the original, however the CDF is still similar to the original CHIRPS and Cultuurtuin CDFs. In other words, resolution has an impact on the QDM transformation process but the impact will not produce considerably different outcomes.

### Extreme precipitation

The reduction of 10% and 5% extremes was to be expected with an average decrease in precipitation in Paramaribo projected by the climate models. 10% and 5% extremes are not that uncommon and thus likely to decrease when the average annual precipitation decreases.

Despite the models projecting lower average annual precipitation, the 0.1% extreme values increase on average. A possible reason is the accompanying future warming in Paramaribo. The air's capacity for water vapor goes up by 7% per degree warming as expected from the Clausius Clapeyron equation, making more intense precipitation events possible (Allan and Soden, 2008). This means that even when the average precipitation decreases, the extreme precipitation can still increase.

The relative changes get higher as the precipitation values become more extreme, going from decreases on average for 10% and 5% extremes to increases on average for 1% and 0.1% extremes.

This is the case for both scenarios and both 1-day and 5-day cumulative precipitation extremes (Figures 26 and 27). The large spread in relative changes in extremes is mainly caused by the large spread for wet models (Figure S.9 and Figure S.10 right, Supplementary Figures). Dry models have a smaller spread and do not contribute to the large spread for all models, apart from the big outlier in the change in 0.1% extremes (Figure S.9 and Figure S.10 left, Supplementary Figures). The figures of the relative changes in extremes separately for dry models and wet models clearly show that the relative changes in extremes increase as the precipitation values become more extreme.

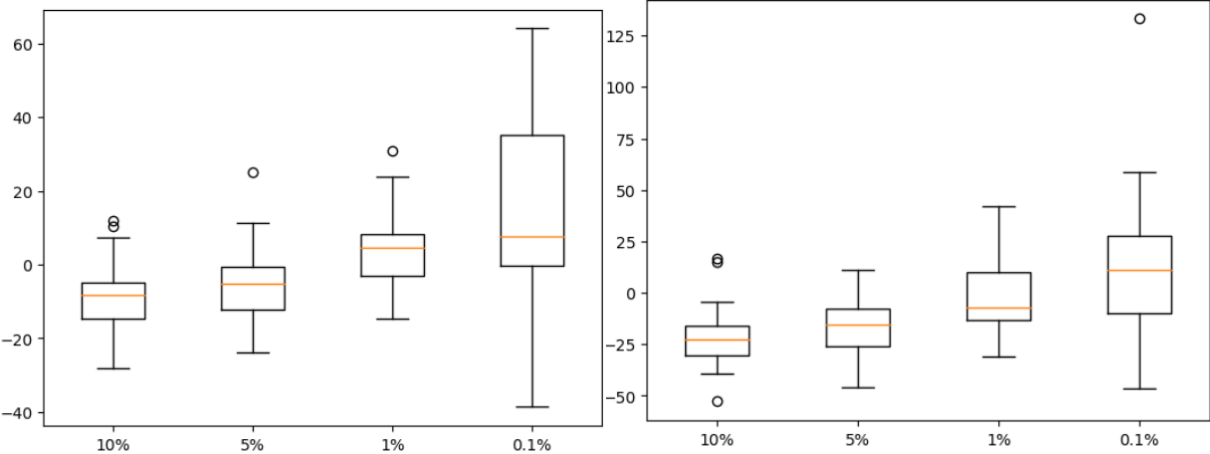


**Figure 26:** Boxplot of relative changes (%), 2085 (2071-2100) – 2005 (1991-2020), in extremes for all models, annual, for 1-day precipitation extremes. SSP2-4.5 (left) and SSP5-8.5 (right).

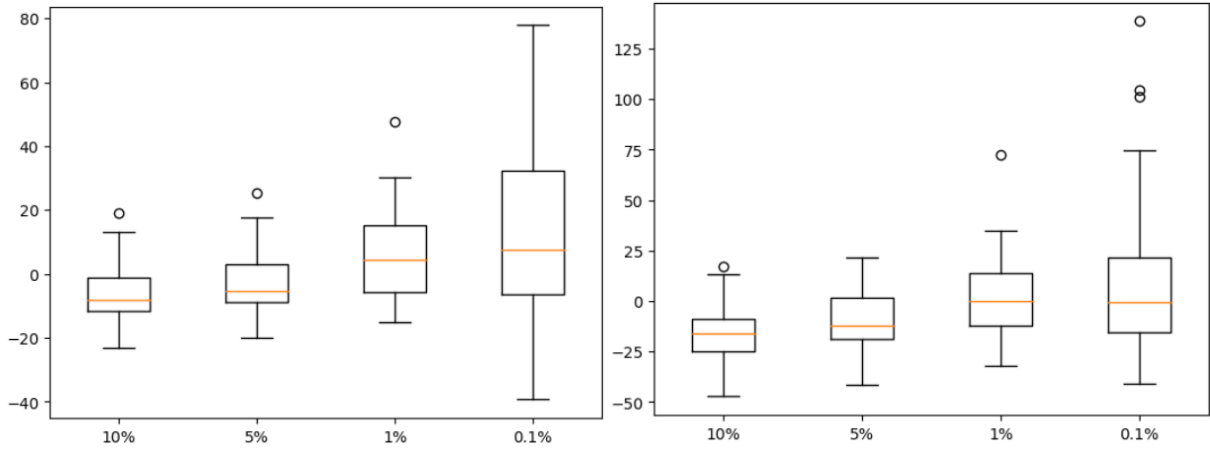


**Figure 27:** Boxplot of relative changes (%), 2085 (2071-2100) – 2005 (1991-2020), in extremes for all models, annual, for 5-day cumulative precipitation extremes. SSP2-4.5 (left) and SSP5-8.5 (right).

## 6. Conclusion

After analysing and discussing the results the research questions from section 1.2. can be answered. The answers to the research questions form the conclusion on the impact of climate change on precipitation in Suriname.

### *1. How well do climate models simulate the climate and observed trends of Suriname?*

By looking at the precipitation bias of historical climate projections in Suriname, it has become clear that the amount of precipitation projected by models is too low in Suriname, especially in the wet season. There is a negative precipitation bias above the equator and a positive precipitation bias below the equator, which means that the position of the Intertropical Convergence Zone (ITCZ) is projected too much to the south in the climate models. In addition, the movement of the ITCZ seems to be 1 month behind in the climate models, with respect to observations.

Improvements in the understanding of the influence of atmospheric processes on the location of the ITCZ would help determining the ITCZ position more accurately by climate models. This will result in better trend observations and climate projections in general.

### *2. Which atmospheric processes influence the climate of Suriname?*

By looking at the multimodel change in time for different variables on a large spatial scale, we found out which atmospheric and oceanic processes have an impact on the climate of Suriname. The processes with the highest impact are the Intertropical Convergence Zone (ITCZ), El Niño Southern Oscillation (ENSO), the Walker Circulation and the Atlantic Meridional Overturning Circulation (AMOC).

The ITCZ moves over Suriname twice a year. The precipitation intensity in Suriname depends mostly on the ITCZ location, with higher precipitation intensity when the ITCZ is located above Suriname.

Weakening of the AMOC results in less warmth being transported from the south Atlantic Ocean to the north Atlantic Ocean, enhancing the warming of the south Atlantic Ocean and cooling of the north Atlantic Ocean. A weakened AMOC leads to a southward shift of the ITCZ in the Atlantic Oceans.

More El Niño like conditions lead to weakening of the mean zonal circulation along the equator and an eastward migration of the Walker Circulation in the Pacific. The occurrence of an increase in upward motion over the Pacific ITCZ and an increase in downward motion over Suriname also indicate an eastward migration of the Walker Circulation. With an eastward migrated Walker Circulation an upward motion of moisture is strengthened and deep convection is increased over the Pacific. At the same time the opposite happens in Suriname where deep convection is decreased due to downward motion of air, with a decrease in precipitation as a result.

3. *What are the causes for the intermodel spread in projected precipitation for Suriname?*

Analyses of differences in projections between models with the most drying in Suriname and models where Suriname gets the least drier or even gets wetter, have been used to find the causes of the intermodel spread in projected precipitation in Suriname. Dry models project the ITCZ more southward than the wet models, which results in the ITCZ being present over Suriname for fewer days and correspondingly less precipitation in Suriname for dry models. One reason for the more southward position of the ITCZ in dry models is a stronger weakening of the AMOC strength in dry models, leading to warming of the south Atlantic Ocean and cooling of the north Atlantic Ocean and thus the ITCZ shifts southward. More El Niño like conditions with a decrease in deep convection in projections from dry models are another reason for lower precipitation projections for dry models than for wet models.

4. *How reliable are the CMIP6 climate projections considering their ability to simulate the actual climate and trends of Suriname and its drivers?*

After the climate models are bias corrected with QDM, the 90% intermodel spread changed from 1-8 mm/day to 4-7.5 mm/day. Next to that, QDM correction has shifted the historical multimodel mean precipitation upwards by approximately 3 mm/day, almost doubling it. The doubling of the average precipitation indicates that climate models fail to accurately project the climate in Paramaribo. The QDM correction significantly improves the climate projections compared to the observations. The large change in historical and future precipitation in Paramaribo after QDM has been applied, suggests that climate models are barely able to simulate the actual climate and trends of Suriname and its drivers.

5. *What are the climate projections for Suriname with respect to downscaled extreme precipitation?*

Due to future warming the 0.1% extremes in Paramaribo increase on average for both 1-day and 5-day cumulative precipitation, as the air capacity for water vapor increases with higher temperature, making more intense precipitation events possible. Lower precipitation extremes like 10% and 5% extremes decrease in value in the climate projections. This is in agreement with the decrease in average precipitation in Paramaribo.

The relative changes in extremes get higher as the precipitation values become more extreme, going from decreases on average for 10% and 5% extremes to increases on average for 1% and 0.1% extremes. This is the case for both scenarios and both 1-day and 5-day cumulative precipitation extremes.

Higher extreme precipitation in the future is concerning with respect to floods in Suriname. With this information, the safety requirements regarding infrastructure, housing, dykes and dams will have to become stricter in Suriname regarding the future.

## **Acknowledgements**

First I would like to thank my supervisors. Martine, thank you for the time and advice you have given me throughout the process of this thesis. The suggestions for the construction of the content and order of the report have helped me a lot in my decisions and have therefore been very important. The attention to detail and clarity helped me to focus on the important aspects of the research. The same goes for Ruud, who, with many critical questions, led me to new insights and directions within the research.

I was kindly received at the KNMI. If I had a question, everyone was ready to help me with my problems right away. The one I want to thank the most is the man who has been the most important during my time at KNMI and helped me every day, Rein Haarsma. Always cheerful and enthusiastic with extensive knowledge of the subjects. Your presence made this period a lot more fun. I also want to thank Emma for the company and the cooperation at the KNMI the past half year. Marta, thank you for taking the time to always answer my questions.

Finally I would like to thank my family and friends for supporting me during my time at TU Delft.

## References

- Alabama Cooperative Extension System. (2021, October 15). *El Niño-Southern oscillation and its impact on Alabama's climate - Alabama Cooperative Extension System*.  
<https://www.aces.edu/blog/topics/crop-production/el-nino-southern-oscillation-and-its-impact-on-alabamas-climate/>
- Allan, R. P., & Soden, B. J. (2008). Atmospheric warming and the amplification of precipitation extremes. *Science*, *321*(5895), 1481-1484.
- Almazroui, M., Islam, M. N., Saeed, S., Saeed, F., & Ismail, M. (2020). Future changes in climate over the Arabian Peninsula based on CMIP6 multimodel simulations. *Earth Systems and Environment*, *4*, 611-630.
- Andreoli, R. V., de Oliveira, S. S., Kayano, M. T., Viegas, J., de Souza, R. A. F., & Candido, L. A. (2017). The influence of different El Niño types on the South American rainfall. *International Journal of Climatology*, *37*(3), 1374-1390.
- Antich-Homar, H., Hess, K., Solaun, K., Alleng, G., & Flores, A. (2022). An Integrated Approach for Evaluating Climate Change Risks: A Case Study in Suriname. *Sustainability*, *14*(3), 1463.
- Bayr, T., Dommenges, D., Martin, T., & Power, S. B. (2014). The eastward shift of the Walker Circulation in response to global warming and its relationship to ENSO variability. *Climate dynamics*, *43*, 2747-2763.
- Bellomo, K., Angeloni, M., Corti, S., & von Hardenberg, J. (2021). Future climate change shaped by inter-model differences in Atlantic meridional overturning circulation response. *Nature Communications*, *12*(1), 3659.
- Brotons, M., Haarsma, R., Bloemendaal, N., de Vries, H., Allen, T. (2023). Drivers of Caribbean precipitation change due to global warming. Analyses and emergent constraint of CMIP6 simulations.
- Brogli, R., Kröner, N., Sørland, S. L., Lüthi, D., & Schär, C. (2019). The role of hadley circulation and lapse-rate changes for the future European summer climate. *Journal of Climate*, *32*(2), 385-404.
- Buckley, M. W., & Marshall, J. (2016). Observations, inferences, and mechanisms of the Atlantic Meridional Overturning Circulation: A review. *Reviews of Geophysics*, *54*(1), 5-63.
- Byrne, M. P., Pendergrass, A. G., Rapp, A. D., & Wodzicki, K. R. (2018). Response of the intertropical convergence zone to climate change: Location, width, and strength. *Current climate change reports*, *4*, 355-370.
- Cai, W., Santoso, A., Collins, M., Dewitte, B., Karamperidou, C., Kug, J. S., ... & Zhong, W. (2021). Changing El Niño–Southern oscillation in a warming climate. *Nature Reviews Earth & Environment*, *2*(9), 628-644.
- Cannon, A. J. (2018). Multivariate quantile mapping bias correction: an N-dimensional probability density function transform for climate model simulations of multiple variables. *Climate dynamics*, *50*, 31-49.
- Cannon, A. J., Sobie, S. R., & Murdock, T. Q. (2015). Bias correction of GCM precipitation by quantile mapping: how well do methods preserve changes in quantiles and extremes?. *Journal of Climate*, *28*(17), 6938-6959.

- Chang, P., Fang, Y., Saravanan, R., Ji, L., & Seidel, H. (2006). The cause of the fragile relationship between the Pacific El Niño and the Atlantic Niño. *Nature*, *443*(7109), 324-328.
- Climate Change Knowledge Database Suriname | Monitoring, Reporting and Verification Tool. (n.d.). <https://dondru.sr/mrv/>
- Climate Model Downscaling – Geophysical Fluid Dynamics Laboratory. (n.d.). <https://www.gfdl.noaa.gov/climate-model-downscaling/>
- Climate variability: North Atlantic oscillation*. (2009, August 30). NOAA Climate.gov. <https://www.climate.gov/news-features/understanding-climate/climate-variability-north-atlantic-oscillation>
- CMIP5 Atmospheric Variables — IPCC-DDC at DKRZ documentation*. (n.d.-b). <https://ipcc-ddc.dkrz.de/doc/ipcc-data/cmip5-variables/index.html>
- cmip6 Data Search | cmip6 | ESGF-CoG*. (n.d.). <https://esgf-node.llnl.gov/search/cmip6/>
- CMIP Phase 6 (CMIP6)*. (2020, February 10). <https://www.wcrp-climate.org/wgcm-cmip/wgcm-cmip6>
- Da Rocha, R. P., Morales, C. A., Cuadra, S. V., & Ambrizzi, T. (2009). Precipitation diurnal cycle and summer climatology assessment over South America: An evaluation of Regional Climate Model version 3 simulations. *Journal of Geophysical Research: Atmospheres*, *114*(D10).
- Delworth, T. L., Zeng, F., Vecchi, G. A., Yang, X., Zhang, L., & Zhang, R. (2016). The North Atlantic Oscillation as a driver of rapid climate change in the Northern Hemisphere. *Nature Geoscience*, *9*(7), 509-512.
- Het klimaat van Suriname - klimaatinfo Suriname*. (n.d.). <https://klimaatinfo.nl/klimaat/suriname/>
- Hirschi, J., Cunningham, S., Bryden, H., & Blaker, A. (2013, April). A new index for the Atlantic Meridional Overturning Circulation at 26N. In *EGU General Assembly Conference Abstracts* (pp. EGU2013-1336).
- Hurrell, J. W., Kushnir, Y., Ottersen, G., & Visbeck, M. (2003). An overview of the North Atlantic oscillation. *Geophysical Monograph-American Geophysical Union*, *134*, 1-36.
- Karmalkar, A. V., Bradley, R. S., & Diaz, H. F. (2011). Climate change in Central America and Mexico: regional climate model validation and climate change projections. *Climate dynamics*, *37*(3), 605-629.
- Köhl, M., Lotfiomran, N., & Gauli, A. (2022). Influence of Local Climate and ENSO on the Growth of *Cedrela odorata* L. in Suriname. *Atmosphere*, *13*(7), 1119.
- Kuhlbrodt, T., Griesel, A., Montoya, M., Levermann, A., Hofmann, M., & Rahmstorf, S. (2007). On the driving processes of the Atlantic meridional overturning circulation. *Reviews of Geophysics*, *45*(2).
- Lee, S. (2014). A theory for polar amplification from a general circulation perspective. *Asia-Pacific Journal of Atmospheric Sciences*, *50*, 31-43.
- Li, H., Sheffield, J., & Wood, E. F. (2010). Bias correction of monthly precipitation and temperature fields from Intergovernmental Panel on Climate Change AR4 models using equidistant quantile matching. *Journal of Geophysical Research: Atmospheres*, *115*(D10).
- Llopart, M., da Rocha, R. P., Reboita, M., & Cuadra, S. (2017). Sensitivity of simulated South America climate to the land surface schemes in RegCM4. *Climate Dynamics*, *49*, 3975-3987.

- Maher, N., Matei, D., Milinski, S., & Marotzke, J. (2018). ENSO change in climate projections: forced response or internal variability?. *Geophysical Research Letters*, *45*(20), 11-390.
- Mastyło, M. (2013). Bilinear interpolation theorems and applications. *Journal of Functional Analysis*, *265*(2), 185-207.
- Matthews, J. R. (2018). Annex I: glossary. *Global warming of, 1*, 541-562.
- McCarthy, G. D., Smeed, D. A., Johns, W. E., Frajka-Williams, E., Moat, B. I., Rayner, D., ... & Bryden, H. L. (2015). Measuring the Atlantic meridional overturning circulation at 26 N. *Progress in Oceanography*, *130*, 91-111.
- McKenna, C. M., & Maycock, A. C. (2021). Sources of uncertainty in multimodel large ensemble projections of the winter North Atlantic Oscillation. *Geophysical Research Letters*, *48*(14), e2021GL093258.
- Mol, J. H., Resida, D., Ramlal, J. S., & Becker, C. R. (2000). Effects of El Niño-related drought on freshwater and brackish-water fishes in Suriname, South America. *Environmental Biology of Fishes*, *59*, 429-440.
- Müller, D., Wip, D., Warneke, T., Holmes, C. D., Dastoor, A., & Notholt, J. (2012). Sources of atmospheric mercury in the tropics: continuous observations at a coastal site in Suriname. *Atmospheric Chemistry and Physics*, *12*(16), 7391-7397.
- Nurmohamed, R., & Naipal, S. (2006). Development of scenarios for future climate change in Suriname. *Acta Nova*, *3*(3), 475-487.
- Nurmohamed, R., Naipal, S., & Becker, C. (2007). Rainfall variability in Suriname and its relationship with the tropical Pacific ENSO SST anomalies and the Atlantic SST anomalies. *International Journal of Climatology: A Journal of the Royal Meteorological Society*, *27*(2), 249-256.
- Nurmohamed, R., Naipal, S., & Becker, C. (2008). Changes and variation in the discharge regime of the Upper Suriname River Basin and its relationship with the tropical Pacific and Atlantic SST anomalies. *Hydrological Processes: An International Journal*, *22*(11), 1650-1659.
- Ortega, G., Arias, P. A., Villegas, J. C., Marquet, P. A., & Nobre, P. (2021). Present-day and future climate over central and South America according to CMIP5/CMIP6 models. *International Journal of Climatology*, *41*(15), 6713-6735.
- Power, S. B., & Smith, I. N. (2007). Weakening of the Walker Circulation and apparent dominance of El Niño both reach record levels, but has ENSO really changed?. *Geophysical Research Letters*, *34*(18).  
*Regridding Overview | Climate Data Guide*. (n.d.). NCAR. <https://climatedataguide.ucar.edu/climate-tools/regridding-overview>
- Santer, B. D., Wigley, T. M., Schlesinger, M. E., & Mitchell, J. F. (1990). Developing climate scenarios from equilibrium GCM results.
- Schneider, T., Bischoff, T., & Haug, G. H. (2014). Migrations and dynamics of the intertropical convergence zone. *Nature*, *513*(7516), 45-53.
- Seager, R., Cane, M., Henderson, N., Lee, D. E., Abernathey, R., & Zhang, H. (2019). Strengthening tropical Pacific zonal sea surface temperature gradient consistent with rising greenhouse gases. *Nature Climate Change*, *9*(7), 517-522.



- Solaun, K., Alleng, G., Flores, A., Resomardono, C., Hess, K., & Antich, H. (2021). State of the Climate Report: Suriname.
- Srokosz, M. A., & Bryden, H. L. (2015). Observing the Atlantic Meridional Overturning Circulation yields a decade of inevitable surprises. *Science*, *348*(6241), 1255-1257.
- Sun, N., Zhou, T., Chen, X., Endo, H., Kitoh, A., & Wu, B. (2020). Amplified tropical Pacific rainfall variability related to background SST warming. *Climate Dynamics*, *54*, 2387-2402.
- Tebaldi, C., & Arblaster, J. M. (2014). Pattern scaling: Its strengths and limitations, and an update on the latest model simulations. *Climatic Change*, *122*, 459-471.
- The collapse of a major Atlantic current would cause worldwide disasters.* (n.d.). World War Zero. <https://worldwarzero.com/magazine/2022/06/the-collapse-of-a-major-atlantic-current-would-cause-worldwide-disasters/>
- Timmermann, A., An, S. I., Kug, J. S., Jin, F. F., Cai, W., Capotondi, A., ... & Zhang, X. (2018). El Niño–southern oscillation complexity. *Nature*, *559*(7715), 535-545.
- Vasconcellos, F. C., Deng, Y., Zhang, H., & Martins, G. (2020). Austral summer precipitation biases over tropical South America in five CMIP5 earth system models. *International Journal of Climatology*, *40*(15), 6506-6525.
- Vauclair, F., & Du Penhoat, Y. (2001). Interannual variability of the upper layer of the tropical Atlantic Ocean from in situ data between 1979 and 1999. *Climate Dynamics*, *17*(7), 527-546.
- Weekes, C., & Bello, O. (2019). Mainstreaming disaster risk management strategies in development instruments (II): policy briefs for Barbados, Guyana, Saint Lucia, Suriname, and Trinidad and Tobago.
- Wikipedia-bijdragers. (2023, January 13). *Suriname*. Wikipedia. <https://nl.wikipedia.org/wiki/Suriname>
- Wilby, R. L., & Dawson, C. W. (2013). The statistical downscaling model: insights from one decade of application. *International Journal of Climatology*, *33*(7), 1707-1719.
- Wills, R. C., Dong, Y., Proistosescu, C., Armour, K. C., & Battisti, D. S. (2022). Systematic climate model biases in the large-scale patterns of recent sea-surface temperature and sea-level pressure change. *Geophysical Research Letters*, *49*(17), e2022GL100011.
- Wood, A. W., Leung, L. R., Sridhar, V., & Lettenmaier, D. P. (2004). Hydrologic implications of dynamical and statistical approaches to downscaling climate model outputs. *Climatic change*, *62*(1-3), 189-216.
- Zhang, R. (2010). Northward intensification of anthropogenically forced changes in the Atlantic meridional overturning circulation (AMOC). *Geophysical Research Letters*, *37*(24).
- Zhuravleva, A., Hüls, M., Tiedemann, R., & Bauch, H. A. (2021). A 125-ka record of northern South American precipitation and the role of high-to-low latitude teleconnections. *Quaternary Science Reviews*, *270*, 107159.

## A Supplementary Figures

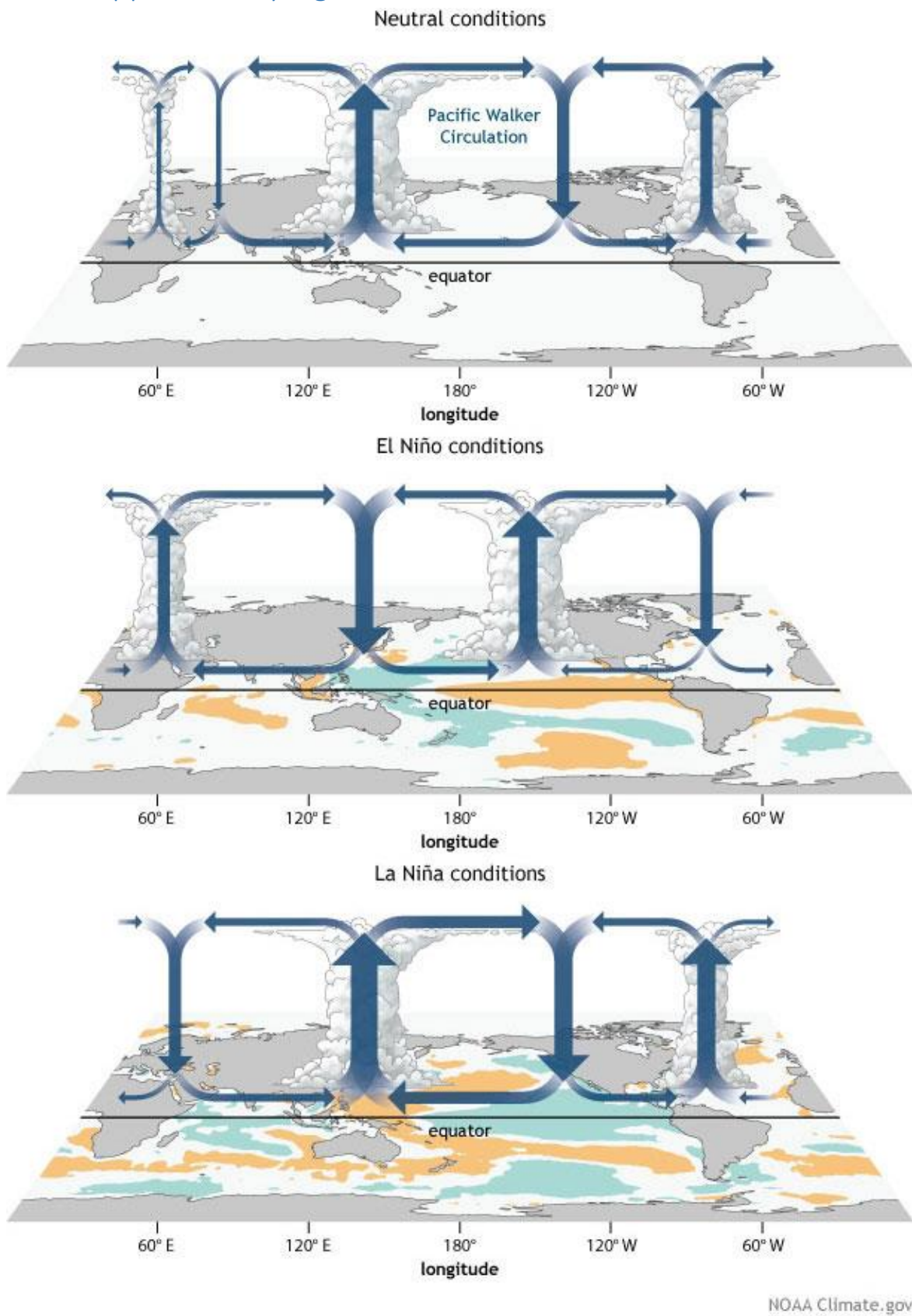


**Figure S.1:** Schematic representation of the zonal tropical atmospheric dynamics for: Neutral conditions, El Niño like conditions and La Niña like conditions. Arrows indicate wind flow. Orange and blue colours represent a positive and negative SST anomaly, respectively. Images from NOAA Climate.

No	CMIP6 model name	Country	Horizontal resolution (lon. by lat. in degree)	Variant label	Key references
1	ACCESS-CM2	Australia	1.9°×1.3°	r1ilplf1	Bi et al. (2012)
2	ACCESS-ESM1-5	Australia	1.9°×1.2°	r1ilplf1	Law et al. (2017)
3	AWI-CM-1-1-MR	Germany	0.9°×0.9°	r1ilplf1	Semmler et al. (2020, in review)
4	BCC-CSM2-MR	China	1.1°×1.1°	r1ilplf1	Wu et al. (2019)
5	CAMS-CSM1-0	China	1.1°×1.1°	r1ilplf1	Rong et al (2019)
6	CanESM5	Canada	2.8°×2.8°	r1ilplf1	Swart et al (2019)
7	CESM2	USA	1.3°×0.9°	r1ilplf1	Lauritzen et al (2018)
8	CESM2-WACCM	USA	1.3°×0.9°	r1ilplf1	Liu et al (2019)
8	CIESM	China	0.9°×1.3°	r1ilplf1	Lin et al. (2020)
10	CNRM-CM6-1	France	1.4°×1.4°	r1ilplf2	Voltaire et al (2019)
11	CNRM-CM6-1-HR	France	0.5°×0.5°	r1ilplf2	Voltaire et al (2019)
12	CNRM-ESM2-1	France	1.4°×1.4°	r1ilplf2	Séférian et al (2019)
13	EC-Earth3	Europe	0.7°×0.7°	r1ilplf1	Massonnet et al. (2020)
14	EC-Earth3-Veg	Europe	0.7°×0.7°	r1ilplf1	Not available
15	FGOALS-f3-L	China	1.3°×1°	r1ilplf1	He et al (2019)
16	FGOALS-g3	China	2°×2.3°	r1ilplf1	Not available
17	FIO-ESM-2-0	China	1.3°×0.9°	r1ilplf1	Song et al. (2020)
18	GFDL-ESM4	USA	1.3°×1°	r1ilplf1	Held et al (2019)
19	INM-CM4-8	Russia	2°×1.5°	r1ilplf1	Volodin et al. (2018)
20	INM-CM5-0	Russia	2°×1.5°	r1ilplf1	Volodin et al. (2018)
21	IPSL-CM6A-LR	France	2.5°×1.3°	r1ilplf1	Not available
22	KACE-1-0-G	South Korea	1.3°×0.9°	r1ilplf1	Not available
23	MIROC6	Japan	1.4°×1.4°	r1ilplf1	Tatebe et al (2019)
24	MIROC-ES2L	Japan	2.8°×2.8°	r1ilplf2	Hajima et al (2019)
25	MPI-ESM1-2-HR	Germany	0.9°×0.9°	r1ilplf1	Gutjahr et al (2019)
26	MPI-ESM1-2-LR	Germany	1.9°×1.9°	r1ilplf1	Mauritsen et al. (2019)
27	MRI-ESM2-0	Japan	1.1°×1.1°	r1ilplf1	Yukimoto et al (2019)
28	NESM3	China	1.9°×1.9°	r1ilplf1	Cao et al (2018)
29	NorESM2-LM	Norway	2.5°×1.9°	r1ilplf1	Seland et al. (2020, in review)
30	NorESM2-MM	Norway	0.9°×1.3°	r1ilplf1	Seland et al. (2020, in review)
31	UKESM1-0-LL	UK	1.9°×1.3°	r1ilplf2	Sellar et al (2019)

**Figure S.2:** List of CMIP6 models with horizontal resolution (longitude and latitude in degrees) (Almazroui et al, 2020).

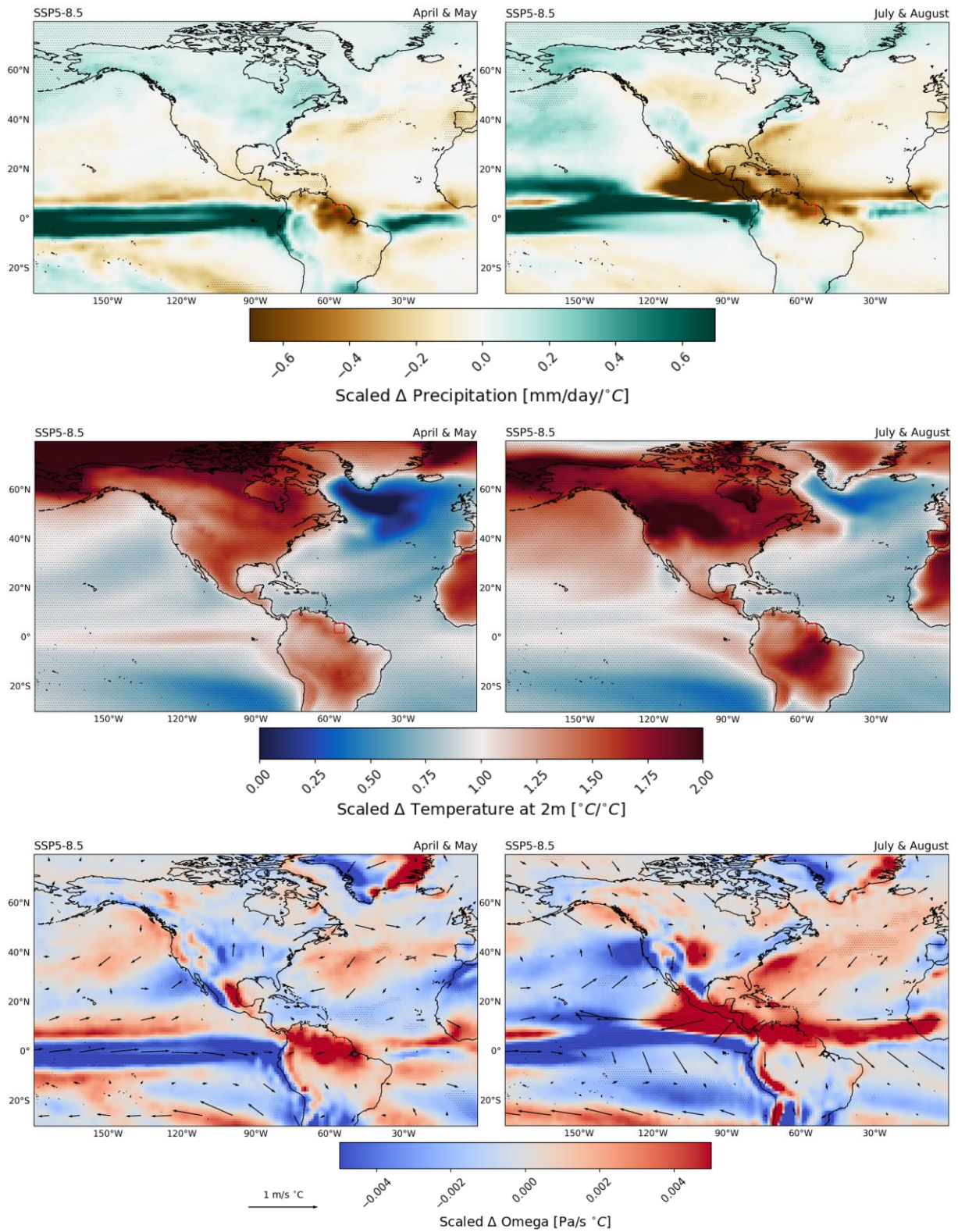


**Figure S.3:** mean scaled change in precipitation, mean scaled change in temperature and mean scaled change in omega at 500 hPa (with wind vectors at 850 hPa) in April & May (left) and July & August (right) for dry models. Hashed regions are significant at a 95% confidence level. Suriname is indicated with the red square.

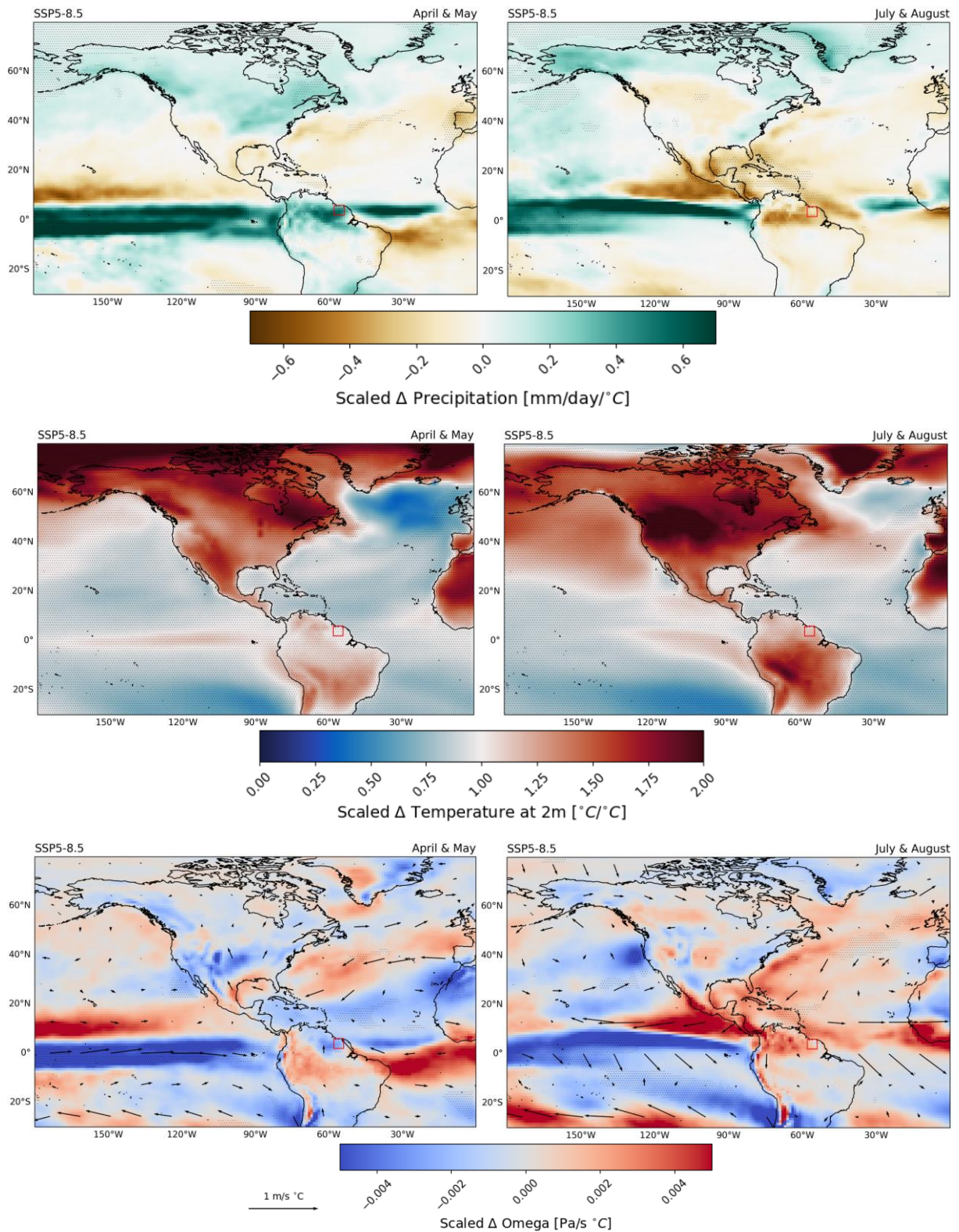


**Figure S.4:** mean scaled change in precipitation, mean scaled change in temperature and mean scaled change in omega at 500 hPa (with wind vectors at 850 hPa) in April & May (left) and July & August (right) for wet models. Hashed regions are significant at a 95% confidence level. Suriname is indicated with the red square.

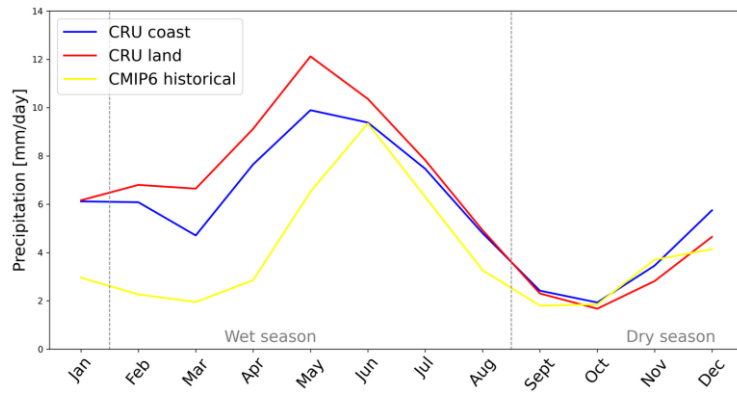


**Figure S.5:** Monthly precipitation in mm/day for historical CMIP multi model mean, CRU coastland and CRU inland.

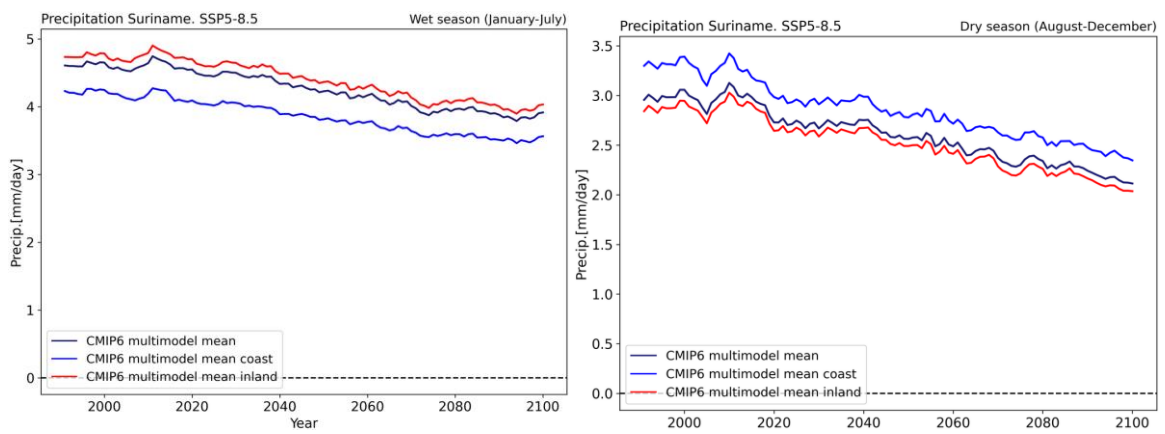


**Figure S.6:** Absolute change in precipitation time series for CMIP6. Suriname, coastland of Suriname and inland of Suriname. Precipitation change in mm/day.

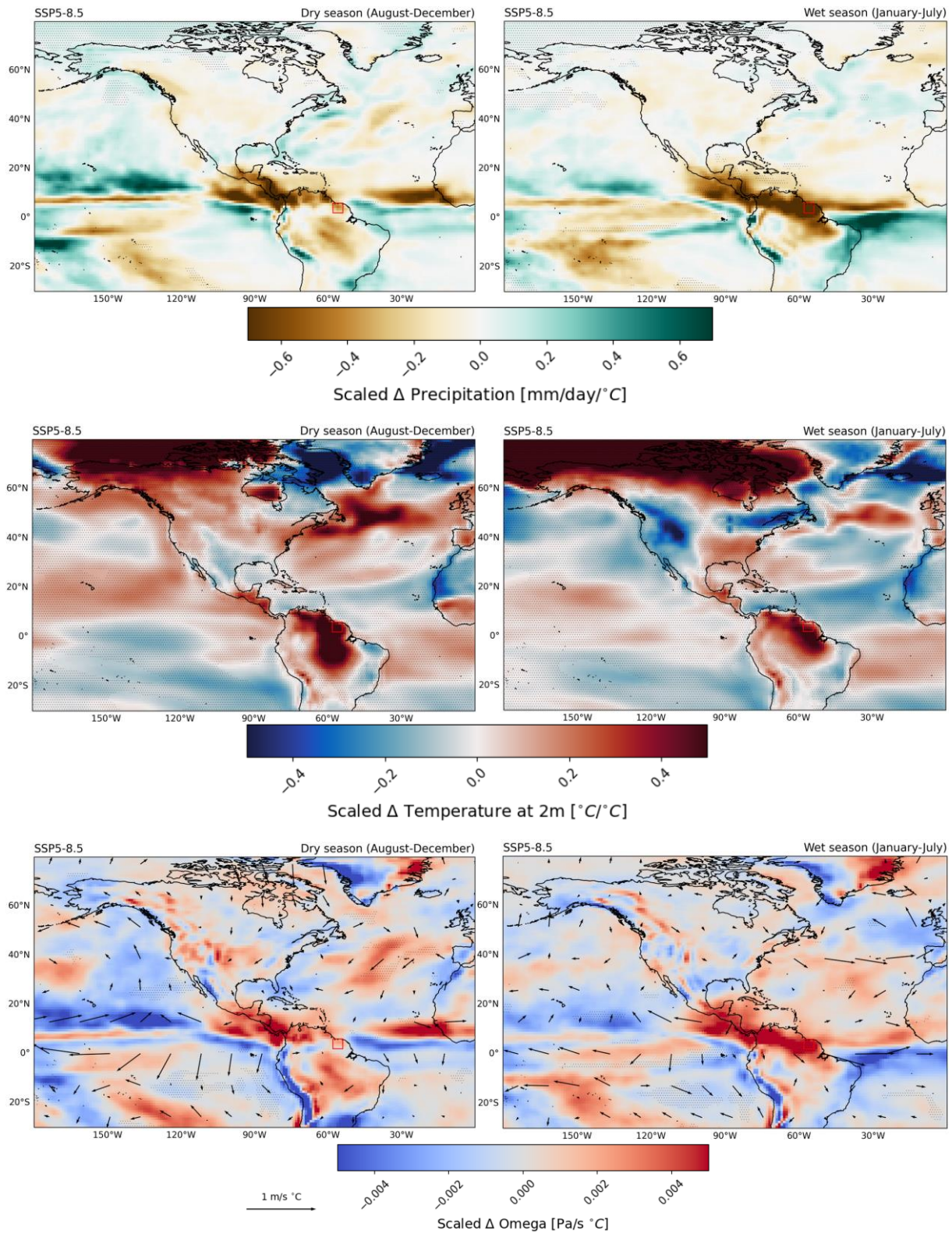


**Figure S.7:** The difference in scaled change in precipitation, temperature and omega at 500 hPa (with wind vectors at 850 hPa) between dry and wet models in  $^{\circ}\text{C}/^{\circ}\text{C}$ . Dry season (left) and wet season (right). Hashed regions are significant at a 95% confidence level. Suriname is indicated with the red square. Three models in the dry group and three models in the wet group.

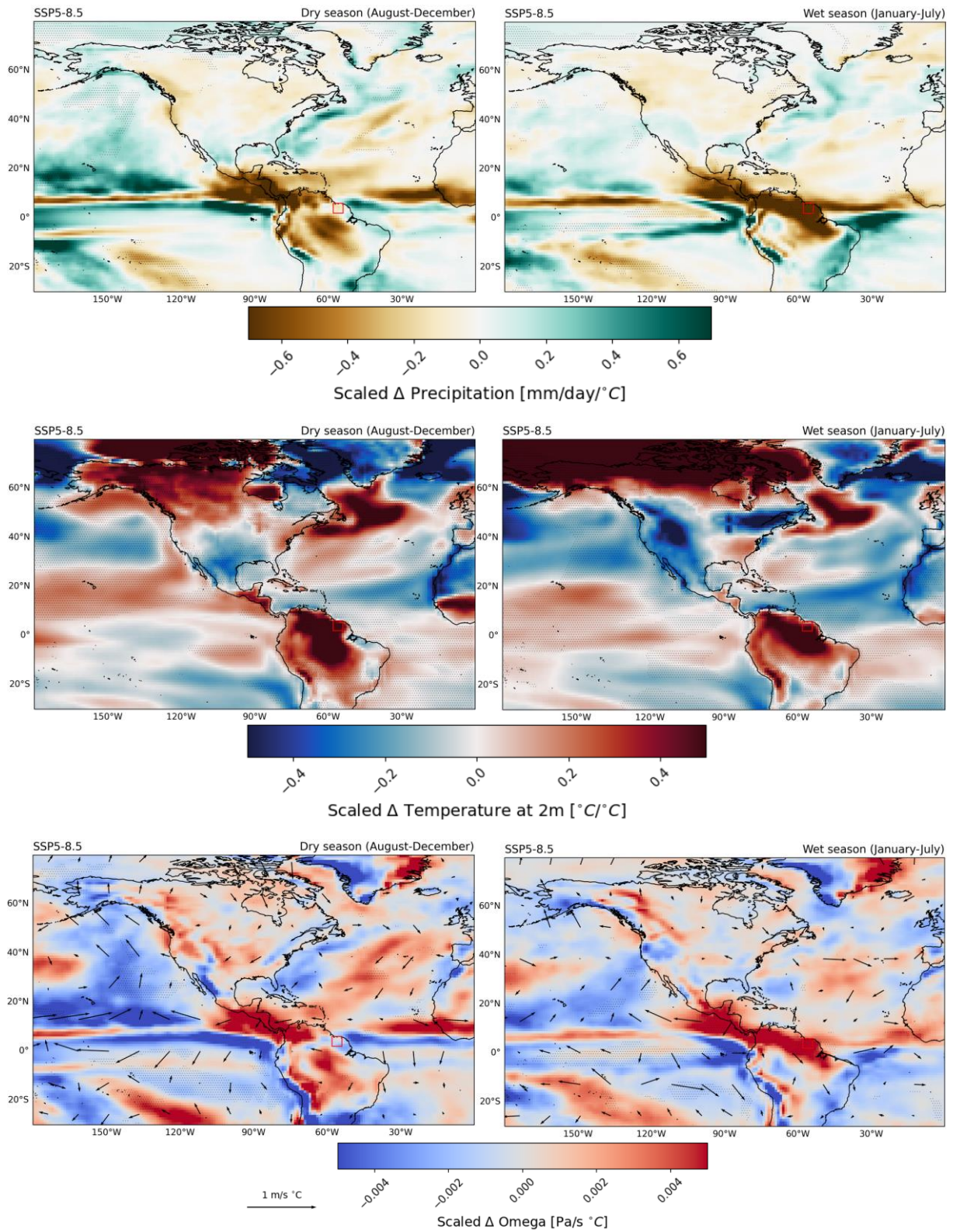


**Figure S.8:** The difference in scaled change in precipitation, temperature and omega at 500 hPa (with wind vectors at 850 hPa) between the two highest increase in precipitation outliers and the two highest decrease in precipitation outliers, for the dry season (left) and the wet season (right). Hashed regions are significant at a 95% confidence level. Suriname is indicated with the red square.



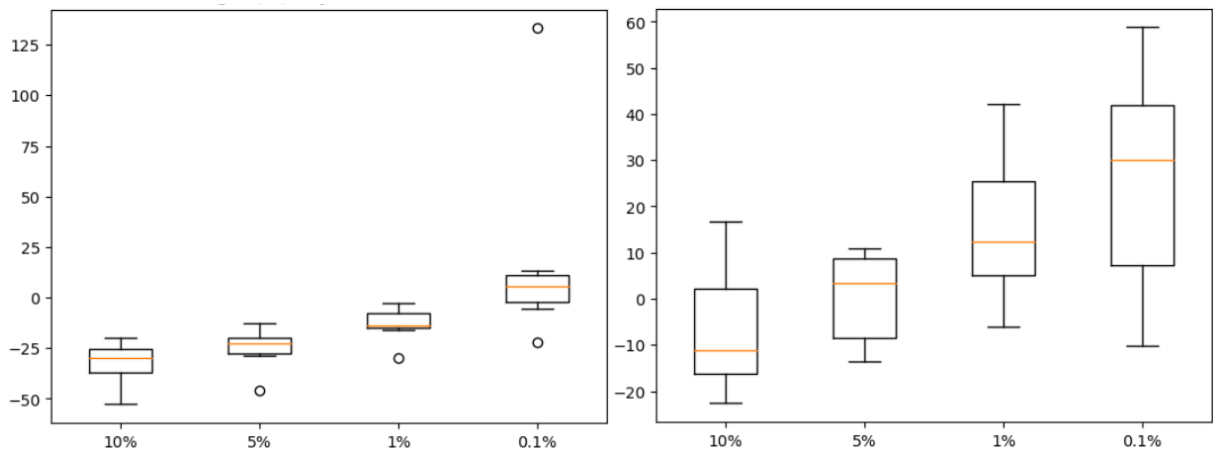


**Figure S.9:** Boxplot of relative changes (%), 2085 (2071-2100) – 2005 (1991-2020), in extremes for dry models (left) and wet models (right), annual, for 1-day cumulative precipitation extremes, scenario SSP5-8.5.

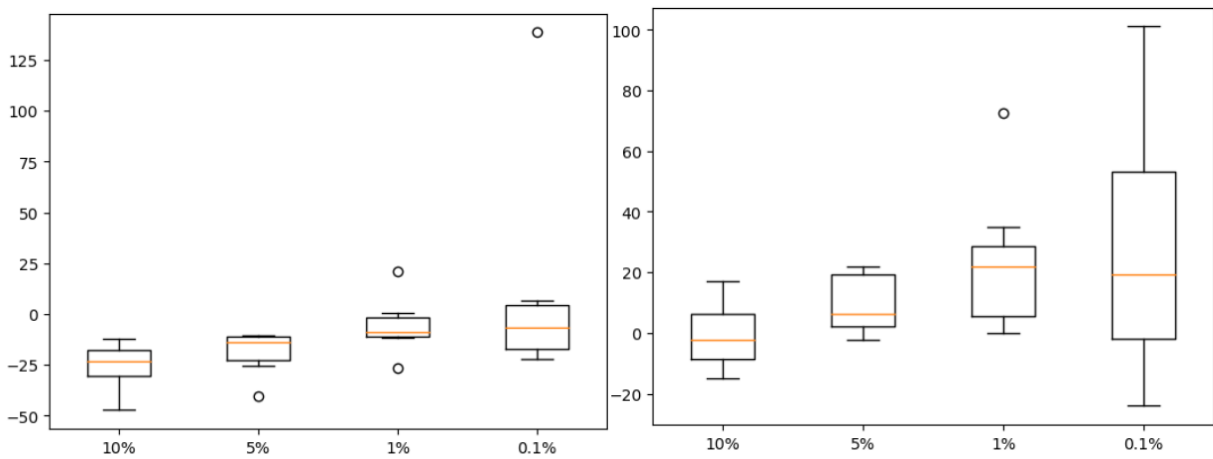


**Figure S.10:** Boxplot of relative changes (%), 2085 (2071-2100) – 2005 (1991-2020), in extremes for dry models (left) and wet models (right), annual, for 5-day cumulative precipitation extremes, scenario SSP5-8.5.

## B Supplementary Tables

	Jan	Feb	Mar	Apr	May	Jun	Jul	Aug	Sep	Oct	Nov	Dec
models historical vs models future	0.199465	0.147196	2.879779e-01	5.455752e-01	4.584674e-01	0.501132	0.030043	0.025465	0.230505	0.367363	0.341033	0.171587
models historical vs GPCP	0.009276	0.000027	2.068037e-08	1.289073e-13	1.507146e-13	0.022074	0.000004	0.000543	0.928281	0.158174	0.000442	0.767213

**Table B.1:** *p*-values for climate models historical (1991-2020) vs climate models future (2071-2100) and climate models historical (1991-2020) vs GPCP values (1991-2020), for every month. *P*-values lower than 0.05 indicate a significant difference between the two compared groups.

	season:	annual				dry season				wet season			
	percentage extremes:	10%	5%	1%	0.1%	10%	5%	1%	0.1%	10%	5%	1%	0.1%
all models	relative change (%)	-8.55	-5.31	2.81	14.28	-8.57	-5.25	0.76	10.42	-8.54	-4.65	3.33	10.49
	absolute change (mm/day)	-1.64	-1.54	1.56	12.10	-1.27	-1.25	0.29	9.90	-1.89	-1.48	2.11	8.00
dry models	relative change (%)	-18.60	-16.24	-6.36	8.01	-20.24	-17.54	-14.68	-3.48	-18.24	-14.13	-3.71	8.09
	absolute change (mm/day)	-3.53	-4.76	-3.60	7.16	-2.88	-3.98	-6.67	-3.21	-4.02	-4.64	-2.28	7.39
wet models	relative change (%)	-4.49	-2.50	7.16	7.77	-8.22	-4.12	3.54	13.43	-4.03	-0.92	5.63	5.92
	absolute change (mm/day)	-0.88	-0.75	3.99	7.02	-1.28	-1.01	1.37	9.00	-0.90	-0.33	3.45	4.64

**Table B.2:** one-day cumulative extreme precipitation for SSP2-4.5. The values represent the mean of the change in extremes of the models. 28 models in all models, seven dry models and seven wet models.

	season:	annual				dry season				wet season			
	percentage extremes:	10%	5%	1%	0.1%	10%	5%	1%	0.1%	10%	5%	1%	0.1%
all models	relative change (%)	-5.78	-2.33	5.15	12.19	-5.65	-3.15	3.30	1.02	-4.89	-0.85	5.44	10.92
	absolute change (mm/day)	-4.76	-2.62	9.07	29.06	-3.55	-2.86	4.30	-7.43	-4.61	-1.02	10.56	27.61
dry models	relative change (%)	-16.18	-12.21	-3.99	2.99	-18.68	-16.76	-14.54	-10.32	-13.19	-8.41	-1.26	-1.09
	absolute change (mm/day)	-13.13	-13.27	-7.52	3.74	-11.26	-14.17	-20.45	-21.29	-12.32	-10.28	-2.99	-10.67
wet models	relative change (%)	-0.93	2.49	4.81	13.58	-3.95	-0.20	5.42	14.34	-0.28	2.71	4.91	18.87
	absolute change (mm/day)	-0.89	2.46	8.83	34.06	-2.67	-0.82	6.03	24.97	-0.38	3.00	9.37	56.46

**Table B.3:** five-day cumulative extreme precipitation for SSP2-4.5. The values represent the mean of the change in extremes of the models. 28 models in all models, seven dry models and 7 wet models.